Stabilization of p53 by microRNAs in HPV-positive cervical cancer cells

Gustavo Martínez-Noël[1,3], Patricia Szajner[1,3], Jennifer A. Smith[1,2], Kathleen Boyland[1], Rebecca E. Kramer[1], and Peter M. Howley[1]*

[1]Department of Immunology, Harvard Medical School, 77 Avenue Louis Pasteur, Boston MA 02115

[2]ICCB-Longwood Screening Facility, Harvard Medical School, 250 Longwood Avenue, Boston MA 02115

[3]These authors contributed equally: Gustavo Martínez-Noël, Patricia Szajner

Abstract word count: 226

Text word count: 10,143

*Corresponding author, Phone: 617-432-2889; Fax 617-432-2882

Email: Peter_howley@hms.harvard.edu

Running Title: HPV p53 miRNA Stabilization Screen

Abstract

Etiologically 5% of cancers worldwide are caused by the high-risk human papillomaviruses (hrHPVs). These viruses encode two oncoproteins (E6 and E7) whose expression is required for cancer initiation and maintenance. Among the cellular targets of these viral oncoproteins are the p53 and the retinoblastoma tumor suppressor proteins. Inhibition of E6-mediated ubiquitylation of p53 through the E6AP ubiquitin ligase results in the stabilization of p53, leading to cellular apoptosis. We utilized a live cell high-throughput screen to assess the ability of 885 microRNAs (miRNAs) to stabilize p53 in human papillomavirus (HPV)-positive cervical cancer cells expressing a p53-fluorescent protein as an *in vivo* reporter of p53 stability. The 32 miRNAs whose expression resulted in the greatest p53 stabilization were further assessed in validation experiments using a second cell-based p53 stability reporter system as well as in HeLa cells to examine their effects on endogenous p53 protein levels. The positive miRNAs identified included 375-3p that has previously been reported as stabilizing p53 in HeLa cells, providing validation of the screen. Additional miRNAs that stabilized p53 led to decreases in E6AP protein levels, while others, including members of the 302/519 family of miRNAs, targeted HPV oncoprotein expression. We further examined a subset of these miRNAs for their abilities to induce apoptosis and determined whether the apoptosis was p53-mediated. The miRNAs described here have potential as therapeutics for treating HPV-positive cancers.

Author summary

Human papillomaviruses cause approximately 5% of cancers worldwide and encode genes that contribute to both the initiation and maintenance of these cancers. The viral gene E6 is expressed in all HPV-positive cancers and functions by targeting the degradation of the p53 protein through its engagement of the cellular ubiquitin ligase E6AP. Inhibiting the degradation of p53 results in apoptosis in HPV-positive cancer cells. We have developed a high-throughput live cell assay to identify molecules that stabilize p53 in HPV-positive cells and we present the results of a screen we have carried out examining miRNAs for their abilities to stabilize p53 and induce apoptosis in HPV-positive cervical cancer cells. These miRNAs have the potential to be used in the treatment of HPV-positive cancers.

Introduction

Cervical cancer is the second leading cause of cancer deaths among women worldwide, with approximately 500,000 new cases diagnosed and 275,000 deaths each year. Virtually all cases of cervical cancer are attributable to infection by HPVs. There are over 200 different HPV types and a subset of these are linked to anogenital tract infections, 14 of which are referred to as hrHPV because they are associated with lesions that can progress to cancer [1]. These same hrHPVs are also associated with other genital tract cancers (penile, vaginal, vulvar, and anal), as well as an increasing number of oropharyngeal cancers. Indeed, approximately 5% of cancers worldwide are caused by HPV [2].

Despite the success of the virus like particle (VLP)-based vaccine that will prevent millions of new HPV-associated cancers, there is the need for effective therapies to treat cancers that will develop in individuals who have not been vaccinated and those already infected

65 with hrHPVs. In this regard, hrHPVs provide a number of potential viral targets for specific
66 HPV antiviral therapies, including the viral encoded oncoproteins E6 and E7, the viral E1
67 helicase, and the viral E2 regulatory protein.
68 The hrHPVs associated with cervical cancer encode two oncoproteins, E6 and E7, that are
69 invariably expressed in HPV-positive cancers and target the important cellular growth
70 regulatory proteins p53 and pRb, respectively [1]. These cancers are dependent upon the
71 continued expression of E6 and E7 and silencing of E6 and E7 expression results in
72 apoptosis and senescence [3, 4]. The E6 proteins of the hrHPV types promote the ubiquitin-
73 dependent degradation of the p53 protein [5] through its binding interaction with the E3
74 ubiquitin ligase E6AP (also known as UBE3A), which ubiquitylates p53 [6-8]. In promoting
75 the ubiquitin dependent proteolysis of p53, E6 counters E7-mediated replication stress
76 signals that activate and stabilize p53 [9]. Thus, inhibition of the E6/E6AP-mediated
77 ubiquitylation of p53 is proapoptotic and provides a potential validated target for HPV-
78 positive cancers. Direct targeting of E6 induces apoptosis in HPV-positive cancer cells [10].
79 Although the hrHPV E6 proteins have other cellular activities and protein targets that have
80 been described in the literature, we have focused on the E6/E6AP pathway as a potential
81 therapeutic target for HPV-positive cancers, as well as precancerous lesions.
82 MicroRNAs (miRNAs/miRs) are small non-coding RNAs (approximately 22 nucleotides in
83 length) that significantly impact and regulate many essential biological pathways. miRNAs
84 negatively regulate gene expression either by translational repression of the target mRNA
85 or cleavage of target mRNAs. Many miRNAs have been shown to play roles in cancer,
86 sometimes as oncogenes and other times as tumor suppressors, making them suitable as
87 therapeutic targets. miRNAs themselves can be used as cancer therapeutics, as their ectopic

88 expression may affect one or more pathways essential for the replication and survival of
89 specific cancer cells. There have been a number of studies focused on HPV and miRNAs in
90 recent years. These studies have examined whether HPVs, like many other viruses, encode
91 viral miRNAs [11] and whether the HPV oncoproteins regulate the expression of cellular
92 miRNAs [12]. Other studies have proposed miRNAs as potential biomarkers of hrHPV
93 infections [13]. There have also been some studies that have examined the effect of miRNA
94 expression in various cancers including cervical cancers (For review see [14]). It was with
95 this mindset, that we conducted a screen to identify miRNAs whose expression in HPV-
96 positive cancer cells would stabilize p53.
97 Here we describe a cell-based platform to assay p53 stability in hrHPV E6-expressing HeLa
98 cells and present our results from a high-throughput screen that identified microRNAs
99 whose expression increased p53 protein levels and caused apoptosis. To our knowledge
100 this is the first study to systematically exam miRNAs for their abilities to stabilize p53 in
101 hrHPV-positive cancer cells. As result of this screen, we have identified a number of
102 miRNAs that when ectopically expressed in these cells lead to increased levels of p53. We
103 also provide insights into the mechanisms by which some of these miRNAs function in
104 stabilizing p53 and apoptosis induction.

105 Results

106 A high-throughput screen identified miRNAs whose
107 overexpression stabilizes p53 in HeLa cells.

108 To identify miRNAs whose overexpression stabilizes p53 and induces apoptosis in hrHPV-
109 positive cancer cells, we performed a high-throughput screen in HPV18-positive HeLa cells
110 harboring a reporter for p53 protein stability. The reporter expresses a bicistronic mRNA
111 that encodes an EGFP-p53 fusion protein and the red fluorescent protein DsRed as
112 reference (Fig 1A). In this screen, we used the p53 gene encoding the R273C mutated
113 protein, which is targeted by E6/E6AP for ubiquitin-dependent proteolysis [15]. This
114 mutant acts as a dominant negative interfering with the transcriptional activities of the
115 endogenous wild-type (wt) p53, thereby preventing p53 transcriptionally-driven apoptosis
116 triggered by the eventual stabilization of the endogenous p53 during the course of the
117 assay. The stability of the EGFP-p53(R273C) fusion protein is controlled by the less stable
118 protein, in this case p53, with a half-life less than 30 minutes in HeLa cells due to E6-
119 mediated proteolysis [5, 16]. To detect changes in p53 stability, we monitored the
120 EGFP/DsRed fluorescence ratio by laser scanning cytometry. The results of this screen,
121 which assayed 885 miRNAs, are shown in S1 Table. The top hit (375-3p) was previously
122 reported to stabilize p53 in HPV-positive cells [17] and thus provided validation for the
123 screen. Of note, since all the miRNAs used in this study are human, we omitted the use of
124 the prefix hsa-miR in the miRNAs names. We selected for further testing the miRNAs that
125 produced the next 32 highest EGFP/DsRed fluorescence ratios (Table 1). Sequence analysis
126 of the selected miRNAs showed a significant enrichment of miRNAs sharing a common seed
127 sequence (5'-AAGUGC-3') that defines the 302-3p/372-3p/373-3p/519-3p/520-3p family
128 of miRNAs (302/519 miRNA family) (S1 Fig). Three additional miRNAs from this family
129 (302d-3p, 520a-3p, and 520e-3p) that had EGFP/DsRed fluorescence ratios close to the
130 selected 32 miRNAs were also included for further evaluation.

131 **Table 1. miRNAs selected from primary screen**

132

Rank	miRNA	Mature_Sequence	EGFP / DsRed (Mean, n = 3)	EGFP / DsRed (SD, n =3)
1	hsa-miR-375-3p	UUUGUUCGUUCGGCUCGCGUGA	0.12298	0.01761
2	hsa-miR-219a-5p	UGAUUGUCCAAACGCAAUUCU	0.07703	0.00559
3	hsa-miR-511-5p	GUGUCUUUUGCUCUGCAGUCA	0.07371	0.00962
4	hsa-miR-519c-3p	AAAGUGCAUCUUUUUAGAGGAU	0.0718	0.0169
5	hsa-miR-943	CUGACUGUUGCCGUCCUCCAG	0.06086	0.02073
6	hsa-miR-200c-5p	CGUCUUACCCAGCAGUGUUUGG	0.05781	0.0079
7	hsa-miR-944	AAAUUAUUGUACAUCGGAUGAG	0.05766	0.03304
8	hsa-miR-106a-3p	CUGCAAUGUAAGCACUUCUUAC	0.0521	0.00779
9	hsa-miR-374b-5p	AUAUAAUACAACCUGCUAAGUG	0.05065	0.00389
10	hsa-miR-148b-5p	AAGUUCUGUUAUACACUCAGGC	0.05013	0.00438
11	hsa-miR-519d-3p	CAAAGUGCCUCCCUUUAGAGUG	0.04929	0.01507
12	hsa-miR-631	AGACCUGGCCCAGACCUCAGC	0.04839	0.01369
13	hsa-miR-592	UUGUGUCAAUAUGCGAUGAUGU	0.0469	0.0122
14	hsa-miR-519b-3p	AAAGUGCAUCCUUUUAGAGGUU	0.04442	0.01903
15	hsa-miR-93-3p	ACUGCUGAGCUAGCACUUCCCG	0.04441	0.00884
16	hsa-miR-340-5p	UUAUAAAGCAAUGAGACUGAUU	0.04336	0.00383
17	hsa-miR-508-3p	UGAUUGUAGCCUUUUGGAGUAGA	0.04083	0.00853
18	hsa-miR-374a-3p	UUAUAAUACAACCUGAUAAGUG	0.03978	0.00887
19	hsa-miR-520d-3p	AAAGUGCUUCUCUUUGGUGGGU	0.0379	0.01428
20	hsa-miR-520c-3p	AAAGUGCUUCCUUUUAGAGGGU	0.0329	0.01176
21	hsa-miR-520b-3p	AAAGUGCUUCCUUUUAGAGGG	0.03226	0.01171
22	hsa-miR-153-3p	UUGCAUAGUCACAAAAGUGAUC	0.03096	0.00799
23	hsa-miR-17-5p	CAAAGUGCUUACAGUGCAGGUAG	0.02945	0.01485
24	hsa-miR-519a-3p	AAAGUGCAUCCUUUUAGAGUGU	0.02878	0.00725
25	hsa-miR-1287-5p	UGCUGGAUCAGUGGUUCGAGUC	0.02854	0.00375
26	hsa-miR-373-3p	GAAGUGCUUCGAUUUUGGGGUGU	0.028	0.00787
27	hsa-miR-302a-3p	UAAGUGCUUCCAUGUUUUGGUGA	0.02791	0.00701
28	hsa-miR-302b-3p	UAAGUGCUUCCAUGUUUUAGUAG	0.02749	0.01175
29	hsa-miR-509-3p	UGAUUGGUACGUCUGUGGGUAG	0.02568	0.00559
30	hsa-miR-210-3p	CUGUGCGUGUGACAGCGGCUGA	0.0256	0.00996
31	hsa-miR-302c-3p	UAAGUGCUUCCAUGUUUCAGUGG	0.02376	0.00492
32	hsa-let-7a-2-3p	CUGUACAGCCUCCUAGCUUUCC	0.02275	0.01039
33	hsa-miR-224-5p	CAAGUCACUAGUGGUUCCGUU	0.0223	0.00997
35	hsa-miR-302d-3p	UAAGUGCUUCCAUGUUUGAGUGU	0.02153	0.00361
42	hsa-miR-520e-3p	AAAGUGCUUCCUUUUUGAGGG	0.01761	0.00714
44	hsa-miR-520a-3p	AAAGUGCUUCCCUUUGGACUGU	0.01673	0.0059

133

134

135 To confirm the results obtained in the screen, we tested the selected miRNAs in HeLa cells
136 containing a different bicistronic reporter vector (Fig 1B) in which p53(R273C) is fused to
137 mRuby, a bright monomeric red fluorescent protein, and the reference monomeric green
138 fluorescent protein SGFP2 is fused to H2B [18]. In this experiment, we determined the
139 percentage of H2B-SGFP2 expressing cells that also expressed mRuby-p53 (R273C) using
140 flow cytometry. We used two randomly selected miRNAs (498-5p and 665), which were
141 negative in the initial screen, and the miRNA Ctrl. 1 as negative controls, along with 375-3p
142 as a positive control. As shown in S2 Fig, 27 of the 32 originally selected miRNAs were
143 confirmed to also stabilize mRuby-p53 (R273C) in this reporter HeLa cell line.

144 Validation of candidate miRNAs in HeLa cells

145 The 27 confirmed miRNAs were next tested for their ability to stabilize endogenous p53 in
146 HeLa cells as determined by western blotting (Figs 2 and S3). While transfection of most of
147 the miRNAs resulted in some degree of p53 stabilization compared to the mock and
148 negative controls, four miRNAs (219-5p, 106a-3p, 592, and 508-3p) had little or no effect
149 on endogenous p53 levels. The other miRNAs ranged from those that produced a mild to
150 moderate increase in p53 levels (511-5p, 519d-3p, 631, 374a-3p, 153-3p, 17-5p, 373-3p,
151 210-3p, and 302c-3p) to those that caused stronger p53 stabilization (519c-3p, 943, 374b-
152 5p, 148b-5p, 519b-3p, 93-3p, 520d-3p, 520c-3p, 520b-3p, 519a-3p, 302a-3p, 302b-3p, 509-
153 3p, and 1287-5p). We also examined the effects of the miRNAs on E6AP and HPV18 E6
154 protein levels. Although most miRNAs had little or no effect on E6AP levels, miRNAs 148b-
155 5p, 374a-3p, and 374b-5p decreased the levels of E6AP to values similar to those observed
156 in cells transfected with the positive control 375-3p, which has been previously shown to
157 target the E6AP mRNA [17]. Transfection of a few miRNAs, most notably 93-3p and 1287-

158 5p, resulted in elevated levels of E6AP (Figs 2 and S3). In contrast, transfection of most of
159 the tested miRNAs led to a reduction in E6 protein levels (Figs 2 and S3). While there was
160 no correlation between the protein levels of E6 and E6AP or between E6AP and p53, there
161 was a significant negative correlation between the levels of E6 and p53, suggesting that a
162 decrease in E6 expression plays a significant role in the stabilization of p53 by several of
163 these miRNAs in HeLa cells (S4 Fig). A ~50% reduction in E6 protein levels appears
164 necessary for p53 stabilization in these cells. Based on these results, we selected miRNAs
165 148b, 374a, 374b, 1287, and five members of the 302/519 family for further analysis.

166 Expression of selected miRNAs increase levels of p53 in 167 different cell lines.

168 To study the effect of this set of miRNAs on the stability of p53 in other hrHPV-positive
169 cancer cell lines, we transfected SiHa (HPV16), ME-180 (HPV68), and MS751 (HPV45) cells
170 with the selected miRNAs and examined p53, E6AP, and actin protein levels by western
171 blot. As shown in Fig 3A-C, the expression of these miRNAs increased the protein levels of
172 p53 in all three cell lines, although with varying efficiencies, indicating that the p53
173 stabilization effect was independent of the hrHPV type.
174 To evaluate the involvement of the E6/E6AP pathway in the stabilization of p53 by these
175 miRNAs, we examined their effects on the levels of p53 and E6AP in HPV-negative human
176 U2OS cells (Fig 3E), an osteosarcoma-derived cell line that harbors wt p53 under the
177 control of Mdm2. Transfection of miRNAs 375-3p and 148b-5p increased the levels of p53
178 in U2OS cells (Fig 3E), indicating that these two miRNAs affect p53 protein levels
179 independent of HPV oncoprotein expression. In contrast, ectopic expression of the miRNAs

180 from the 302/519 family and 1287-5p had no effect on the levels of p53 in U2OS cells,
181 suggesting that the effect of these miRNAs on p53 stability depends on the expression of
182 hrHPV E6. Of note, transfection of miRNAs 375-3p, 148b-5p and to a lesser degree 374a-3p
183 and 374b-5p, decreased the levels of E6AP in each of the cell lines analyzed. As expected,
184 no miRNA produced a significant change in p53 levels in the HPV-negative C33A cervical
185 cancer cell line that already expresses high levels of an inactive mutant form of p53 (Fig
186 3D) [19].
187 Since transfection of the 302/519 family members and 1287-5p miRNAs only increased
188 p53 levels in HPV-positive cells and led to decreased E6 protein levels in HeLa cells, which
189 negatively correlated to the levels of p53 (Figs 2 and 4S), we hypothesized that the ability
190 of these miRNAs to stabilize p53 in HPV-positive cancer cells was a direct consequence of
191 their effect on E6 expression. This could be a consequence of destabilizing the E6 protein,
192 targeting the E6/E7 mRNAs for degradation or sequestration, or decreasing viral
193 transcription. To explore these possibilities, we examined the effect of the miRNAs on the
194 levels of p53 in 1321 cells, a human keratinocyte cell line that expresses HPV16 E6/E7
195 under the control of the human β-actin promoter and from a mRNA with the 3'
196 untranslated region (3'UTR) of the human β-actin mRNA [20] (Fig 3D). While transfection
197 of miRNAs 375-3p, 148b-5p, 374a-3p, and 374b-5p stabilized p53, ectopic expression of
198 miRNAs of the 302/519 family and 1287-5p produced little to no change on p53 levels in
199 1321 cells. This indicates that stabilization of p53 by the miRNAs of the 302/519 family
200 and 1287-5p in HPV-positive cervical cancer cell lines is likely mediated by reduced E6
201 expression from the viral long control region (LCR) promoter.

202 **Several miRNAs repress the promoter activity of the HPV16 and**

203 **18 LCRs.**

204 The hrHPV E6 and E7 genes are expressed from a single promoter located in the viral LCR.
205 Consistent with the hypothesis that these miRNAs affect the promoter activity of the viral
206 LCRs, we observed that their transfection into HeLa cells, particularly the members of the
207 302/519 family and 1287-5p, decreased both E6 and E7 protein levels similarly (Fig 4A).
208 To examine whether these selected miRNAs repressed promoter activity of the HPV LCRs,
209 we used reporter plasmids that express firefly luciferase under the control of either the
210 HPV16 or HPV18 LCR (Fig 4B). Remarkably, with the exception of 148b-5p, all of the
211 miRNAs tested repressed the LCR-dependent expression of firefly luciferase in C33A cells.
212 Most miRNAs showed a comparable effect on both LCRs, except 374b-5p, which did not
213 significantly repress the HPV16 LCR. Expression of the 302/519 family members and 1287-
214 5p led to the greatest repression of both HPV16 and HPV18 LCRs.
215 We next used qRT-PCR to directly assess the impact of these miRNAs on the levels of HPV
216 E6/E7 mRNAs in HeLa and SiHa cells (Fig 4C). Using primers that detect all HPV E6/E7
217 transcripts, we observed a significant reduction of the E6/E7 mRNAs upon transfection
218 with each of the miRNAs except 148b-5p in HeLa cells, indicating regulation of E6 and E7
219 expression at a pre-translational level. Although 498-5p reduced the level of the E6/E7
220 mRNAs in HeLa cells, consistent with the reduced level of E6 protein shown in Fig 2, we did
221 not observe an increase in p53 protein levels in these cells (see discussion). While 375-3p
222 was equally efficient in repressing the expression of the E6/E7 mRNAs in both HPV-
223 positive cell lines, most of the tested miRNAs were less efficient in SiHa than in HeLa cells

224 even though SiHa cells were efficiently transfected as determined by siGlo RISC-free
225 transfection control (Horizon). Surprisingly, transfection of 148b-5p increased the level of
226 the E6/E7 mRNAs in both cell lines suggesting that neither downregulation of the
227 promoter activity of the LCR nor destabilization of the E6/E7 mRNAs contribute to the
228 stabilization of p53 by this miRNA in these cells. We also observed that transfection of 375-
229 3p, which efficiently reduced the E6/E7 mRNAs levels in both HeLa and SiHa cells, has a
230 milder effect on both viral promoters compared to the miRNAs of the 302/519 family or
231 1287-5p, indicating that, as published by others, 375-3p also affects the levels of the E6/E7
232 mRNAs post-transcriptionally [17]. A similar observation can be made for 374a-3p and
233 374b-5p in HeLa cells. In general, in HeLa cells, there is a correlation between the levels of
234 E6 protein and E6/E7 mRNAs with the degree of repression of the viral promoter,
235 suggesting that downregulation of the LCR promoter is an important factor in the
236 regulation of E6 expression by the tested miRNAs in these cells. In contrast, in SiHa cells,
237 with the exception of 148b-5p, there was little or no correlation between the levels of the
238 E6/E7 mRNAs and the degree of repression of the viral promoter. This indicates that, in
239 addition of repressing the LCR promoter activity, other factors likely contribute to the E6
240 downregulation and p53 stabilization by these miRNAs in SiHa cells.

241 miRNAs of the 302/519 family and 1287-5p induce p53-
242 dependent apoptosis in HeLa cells.

243 Stabilization of p53 is expected to be pro-apoptotic in hrHPV-positive cells. We therefore
244 tested the miRNAs that stabilized p53 in HeLa cells for their abilities to induce apoptosis.
245 Flow cytometry analysis of HeLa cells transfected with different miRNAs and stained with

246 the apoptosis marker Annexin V revealed an increase in the fraction of apoptotic cells when
247 compared to untreated or mock transfected cells (Fig 5). Surprisingly, miRNAs Ctrl.1 and
248 498-5p, which did not increase p53 levels in hrHPV positive cells (Figs 2 and 3) also led to
249 an increase in Annexin V staining in HeLa cells. In addition, we noticed a strong correlation
250 between induction of apoptosis, stabilization of p53 (Fig 2), and repression HPV18 LCR (Fig
251 4B) in HeLa cells transfected with the 302/519 family members. In this family, 519d-3p,
252 which produced the lowest increase in p53 level in HeLa cells, was also the least efficient in
253 inducing apoptosis.
254 We next examined the ability of a subset of these miRNAs to induce apoptosis in SiHa cells
255 and two HPV-negative cancer cell lines, C33A and U2OS, using Annexin V staining (Fig 6).
256 Because the negative controls Ctrl. 1 and 498-5p induced apoptosis in HeLa cells (Fig 5), we
257 included the miRNA 20a-3p as a negative control since it has been previously reported not
258 to induce apoptosis in cervical cancer cells [21]. The 1287-5p miRNA was also included in
259 these experiments as it was found to stabilize p53 (Figs 2 and 3) and efficiently repressed
260 the E6/E7 mRNAs expression in HeLa and SiHa cells as well as the promoter activity of the
261 HPV16 and HPV18 LCR reporters (Fig 4B and 4C). Similar to our results in HeLa cells,
262 148b-5p and 1287-5p induced apoptosis in SiHa cells whereas 375-3p and 519b-3p had
263 very little or no effect (Fig 7). All of these miRNAs increased the levels of p53 when
264 transfected into SiHa cells (Fig 3A); however, 148b-5p and 1287-5p led to the highest p53
265 levels. Both 148b-5p and 1287-5p stimulated apoptosis in C33A cells indicating that these
266 miRNAs can induce apoptosis independently of p53.
267 We next examined the requirement for p53 stabilization in the induction of apoptosis in
268 HeLa cells for several representative miRNAs. We performed Annexin V staining of HeLa

269 cells co-transfected with the miRNAs and an siRNA targeting p53 or its C911 variant [22] to
270 address possible off-target effects of the siRNA (Fig 7A). As expected, the positive control
271 375-3p increased the percentage of Annexin V-stained cells while 20a-3p had no significant
272 effect when compared to untreated cells. Surprisingly, the apoptotic effect of 375-3p was
273 independent of p53 since knock-down of p53 had little effect on the percentage of
274 apoptotic cells in HeLa cells co-transfected with this miRNA. The effect of 498-5p on
275 apoptosis is also p53-independent and consistent with the inability of this miRNA to
276 stabilize p53 when transfected into hrHPV-positive cell lines (Figs 2 and 3). Similarly, the
277 apoptotic effects of miRNAs 148b-5p and 374a-3p are p53-independent, as co-transfection
278 of these miRNAs with either the siRNA against p53 or its C911 version have similar effects
279 on the percentage of apoptotic cells. This indicates that, in these cases, the effect observed
280 when p53 is knocked down can be attributed to off-target effects of the siRNA against p53.
281 In contrast, the numbers of apoptotic cells observed with 519b-3p (as a representative of
282 the 302/519 family of miRNAs) and 1287-5p were reduced when co-transfected with the
283 p53 siRNA but not with its C911 version, indicating that the apoptotic effect of these
284 miRNAs is largely p53-dependent in HeLa cells. Similar results were obtained when using
285 PARP cleavage as a marker for apoptosis in western blot analysis (Fig 7B). Altogether,
286 these results showed that expression of the selected miRNAs induces apoptosis in HeLa
287 cells via mechanisms that are either independent of p53 protein levels, as in the case of
288 148b-5p and 374a-3p, or p53-dependent, as found with 519b-3p and 1287-5p.

289 # Discussion

290 In this manuscript, we describe a platform that can be used in a high-throughput manner
291 (e.g. siRNA, CRISPR-Cas9, and small molecule screens) to monitor p53 stability *in vivo* in
292 HPV-positive cancer cells. Here we present our results using this platform to screen a
293 library of miRNA mimics in HeLa cells to find candidates whose overexpression stabilized
294 p53 in hrHPV-positive cancer cells. We identified several miRNAs that increased the
295 protein levels of p53 when transfected in HeLa cells. Some of these miRNAs (148b-5p,
296 302a-3p, 373-3p, and 374b-5p) have been reported to be expressed at lower levels in
297 cervical cancer cells and tissues compared to the controls used in each of the studies [21,
298 23-25]. In contrast, 1287-5p has no change in its expression level in cervical cancer cells,
299 but is sequestered from its targets by the circular RNA circSLC26A4, which is
300 overexpressed in hrHPV-positive cancer cells [26]. In addition, some of the miRNAs
301 identified in our screen, namely 148b-5p, 302a-3p, 374b-5p, or 519b-3p, have already been
302 shown to have effects in hrHPV-positive cervical cancer cells affecting cellular behavior,
303 slowing cell growth and inducing apoptosis [23-25, 27, 28]. Although several targets and
304 mechanisms have been shown to contribute to these effects, there is little data about how
305 the ectopic expression of these miRNAs affects E6, E6AP and p53 expression, nor the
306 possible consequences of changes in the expression E6, E6AP, and p53 in the ability of
307 these miRNAs to induce apoptosis in hrHPV-positive cervical cancer cells.
308 Since the ubiquitin ligase activity of E6AP/E6 is responsible for the efficient ubiquitin-
309 dependent proteolysis of p53 in hrHPV-positive cervical cancer cells, we checked the levels
310 of E6AP in cells transfected with the different miRNAs. Interestingly, only four miRNAs,
311 148b-5p, 374a-3p, 374b-5p, and 375-3p, were identified that led to a decrease in E6AP

312 protein levels. Remarkably, the three miRNAs of this group that were further analyzed
313 (148b-5p, 374a-3p, and 375-3p) increased apoptosis in HeLa cells in a p53-independent
314 manner. It is possible that this induction of apoptosis may still be HPV-related, as these
315 miRNAs also led to decreased E6 protein expression. However, 148b-5p induced apoptosis
316 in the absence of the HPV oncoproteins as observed in C33A cells and both 375-3p and
317 148b-5p stabilized p53 in HPV-negative U2OS cells. These results indicate that these
318 miRNAs can affect p53 protein levels independent of their effect on E6. Although we did not
319 determine whether they directly target the E6AP mRNA, it seems probable for both 148b-
320 5p and 374b-5p because target prediction analysis using the miRDB database
321 (www.mirdb.org) [29, 30] revealed that each has three sites complementary to their seed
322 sequences within the 3'UTR of the E6AP mRNA. They start at positions 395, 664, and 1595
323 of the 3'UTR for 148b-5p, and at positions 236, 908, and 1334 for 374b-5p.
324 In contrast, our results indicate that 519b-3p (member of the 302/519 family) and 1287-
325 5p induce apoptosis in HeLa cells in a p53-dependent manner. Our observations do not
326 fully align with previous reports that indicated transfection of 519b-3p increases p21 levels
327 in a partly p53-independent manner, resulting in growth inhibition and cell survival, while
328 failing to induce cell death [28]. There are a number of technical differences between our
329 study and that of Abdelmohsen et al. which could account for the discordant results.
330 Different concentrations of miRNAs were used in each study (50 nM in the Abdelmohsen
331 study and 10 nM in our study) and their analyses were done at 48 hours post-transfection
332 whereas our studies were conducted at 72 hours post transfection.
333 Although there are sequences complementary to the seed sequence of miRNAs of the
334 305/519 family in the 3'UTR of the E6AP mRNA (starting at positions 934 and 935 of the

335 3'UTR) we did not observe any significant effect on E6AP expression levels in the various
336 cell lines transfected with these miRNAs. However, it has recently been reported that 302c-
337 3p, which belongs to this family, regulates the expression of E6AP by targeting the 3'UTR of
338 the E6AP mRNA in hepatic stellate cells [31]. Again, methodological differences between
339 the two studies, most notably the cell type used, could explain the different findings. It is
340 feasible that the cells differ in availabilities of the target sequence in the 3'UTR of the E6AP
341 mRNA for the miRNAs of the 302/519 family, for example by differential expression of an
342 RNA-binding protein that could compete with the miRNAs for binding to the target
343 sequence [32]. In addition, the concentration of miRNA used by Kim et al. was 100 nM, ten
344 times higher than that used in our study. Overexpression of miRNAs can produce a series of
345 confounding effects (reviewed in [33]), such as binding to lower-affinity targets that are
346 not affected by lower miRNA concentrations. At a concentration of 10 nM we found that the
347 miRNAs of the 302/519 family stabilize p53 but do not impact E6AP expression in cervical
348 cancer cells. The fact that they can stabilize p53 at relatively low concentrations makes
349 them more attractive as potential therapeutics for cervical cancer by reducing potential
350 side effects due to targeting of low affinity sites.
351 Different viral processes affected by host miRNAs have been described (reviewed in [34]);
352 however, miRNAs affecting the activity of viral promoters are not commonly found in the
353 literature. Transfection of 302/519 family members or 1287-5p led to increased protein
354 levels of p53 only in cells in which E6 and E7 expression is driven by viral LCRs (HeLa,
355 SiHa, ME-180, and MS751). This suggests that the effect of these miRNAs on E6 and E7
356 expression may involve a reduction in the activity of the viral promoters. Here we showed
357 that ectopic expression of these miRNAs efficiently repressed the activity of the HPV16 and

358 HPV18 LCRs in C33A cells expressing LCR/luciferase reporters and resulted in decreased
359 E6/E7 mRNAs levels in both HeLa and SiHa cells. It is possible that these miRNAs target
360 transcription factors that regulate HPV LCR promoter activities. We note that although
361 375-3p has been reported to target E6/E7 mRNAs in HeLa and SiHa cells [17], our data
362 show that 375-3p also decreases the expression levels of E6 and E7 by repressing the
363 promoter activity of the viral LCRs. This might involve the downregulation of the
364 transcription factor SP1 by 375-3p [35], which is key for the activity of the promoter
365 driving E6 and E7 expression in hrHPVs [36, 37]. In terms of the 302/519 miRNA family
366 members, 519a-3p and 519d-3p have been shown to target signal transducer and activator
367 of transcription 3 (STAT3) mRNA [38, 39], which is another driver of HPV gene expression
368 [40]. Noteworthy, knocking down or inhibiting STAT3 in hrHPV-positive cervical cancer
369 cell lines led to loss of E6 and E7 expression, accumulation of p53, and reduced cell viability
370 [41]. The similarities between the effects of ectopic expression of the 302/519 family of
371 miRNAs and STAT3 depletion in hrHPV-positive cancer cells make STAT3 an interesting
372 candidate to mediate the effects of these miRNAs in hrHPV-positive cells. Another
373 possibility is that these miRNAs regulate the LCR promoter activity through direct binding
374 to viral or host DNA as it has been described for other miRNAs [42]. Though we could not
375 find any evident sequence similarities to these miRNAs in the HPV16 and HPV18 genomes,
376 we cannot fully exclude this possibility. These are all interesting questions that will be
377 addressed in future studies.
378 Both the 302/519 family members and 1287-5p induced apoptosis in HeLa cells. In the
379 case of 519b-3p (as representative of the 302/519 family of miRNAs) and 1287-5p this
380 induction was p53-dependent. Surprisingly, 519b-3p failed to induce apoptosis in SiHa

381 cells despite increasing the levels of p53. It has been previously reported that p53 must
382 accumulate to a threshold level to induce apoptosis [43]. Thus, it is feasible that for 519b-
383 3p the concentration of miRNA and/or incubation times used in this study did not increase
384 p53 levels enough to reach the critical threshold necessary to trigger apoptosis in SiHa
385 cells. A similar reasoning could be applied to 148b-5p, which failed to induce apoptosis in
386 U2OS cells despite the stabilization of wt p53 (Fig 3E). In contrast, 1287-5p induced
387 apoptosis in U2OS cells without a noticeable increase in p53 levels, indicating that in these
388 cells this miRNA promotes cell death independent of p53 stabilization. This suggests that
389 1287-5p can induce apoptosis via different pathways depending on cell type, highlighting
390 the risk of extrapolating miRNA effects observed in one cell line to different cell types. Of
391 note, transfection of 498-5p, which was initially chosen as a negative control because it did
392 not stabilize p53 in HeLa cells, resulted in decreased levels of E6 in these cells. This
393 suggests that either the remaining E6 protein was sufficient to target p53 for degradation
394 or that 498-5p has the additional property of inhibiting p53 accumulation. However, in this
395 study, the miRNAs that failed to reduce E6 protein levels to approximately half of its
396 original amount or beyond also failed to increase p53 levels in HeLa cells, suggesting that
397 there is a considerable excess of E6 in these cells that must be overcome in order to
398 stabilize p53. Interestingly, ectopic expression of Ctrl. 1 stabilized p53 only in U2OS cells,
399 further demonstrating how an individual miRNA affects different cell types in distinct
400 ways.
401 A match of the seed sequence of the miRNAs is very important for target recognition [44,
402 45]. However, it has been reported that additional pairing to 3' sequences of miRNAs
403 frequently participate in target site recognition and avidity, resulting in different target

404 specificities for miRNAs of a given miRNA family [46]. In this study we found that different
405 members of the 302/519 family of miRNAs, all with the same seed sequence, differed in the
406 extent to which p53 protein levels increased, indicating that 3' miRNA sequences may also
407 play a role in their stabilization of p53 in hrHPV-associated cancer cells. Regardless, the
408 common seed sequence of the miRNAs within the 302/519 family that we found to repress
409 the HPV18 and HPV16 LCR promoters is a characteristic that can be used to identify their
410 potential targets involved in viral LCR promoters regulation.
411 Since their discovery in 1993 [47, 48], there has been a major and growing interest in
412 miRNAs. A PubMed search for articles with "microRNA" or "miRNA" in the title reveals
413 more than 41,000 publications. Research in miRNAs is being translated into diagnostics as
414 miRNAs are considered sensitive and specific biomarkers whereas therapeutic
415 opportunities with miRNAs have lagged with only a few clinical trials currently in progress
416 (reviewed in [49, 50]). This may in part be due to the lack of single target specificity
417 characteristic of miRNAs. This multiplicity of targets makes miRNAs potentially challenging
418 as therapeutics because of the possibility of unexpected and/or undesirable side effects.
419 However, this property makes them an attractive tool for cancer treatment since miRNAs
420 can simultaneously regulate multiple cellular pathways by modulating the expression of
421 several genes in a coordinated fashion. The utility of miRNAs as therapeutic tools will be
422 improved by a more complete understanding of how they function in the cellular networks
423 in which they are embedded. In this study, we identified several miRNAs that stabilize p53
424 and can induce apoptosis, both in a p53-dependent or p53-independent manner, when
425 ectopically expressed in hrHPV-positive cancer cells. Most of these miRNAs function
426 through transcriptional repression of the HPV LCR promoter, especially 519b-3p and 1287-

427 5p. Further research on the mechanisms used by these miRNAs to repress the hrHPV LCRs
428 and induce apoptosis in HPV-positive cervical cancer cells will improve our understanding
429 of the hrHPV-host interactions and possibly contribute to the identification of new
430 therapeutic targets for hrHPV infections and cancers.

431 Materials and methods

432 Plasmids

433 To create a lentiviral reporter vector to monitor the protein levels of p53 *in vivo* in hrHPV
434 cancer cells, the p53 open reading frame (ORF) carrying the mutation R273C was first
435 amplified by PCR using the primers hp53-1 (5'-CACCATGGAGGAGCCGCAGTCAGATCC-3')
436 and hp53-8 (5'-GGATCCTCAGTCTGAGTCAGGCCCTTCTGTCTTG-3') and cloned into the
437 pENTR/D-TOPO vector (ThermoFisher) generating the entry vector pENTR p53(R273C)
438 (p6140). The p53(R273C) ORF was then recombined from the entry vector into a lentiviral
439 vector containing a GPS (Global Protein Stability) cassette (gift from S. Elledge) using the
440 GATEWAY cloning system (ThermoFisher), resulting in the vector pHAGE-P CMVt N-RIG2
441 p53(R273C) (p7987). The GPS reporter cassette expresses a bicistronic mRNA encoding
442 EGFP fusion proteins and the red fluorescent protein DsRed as reference (Fig 1A) [51-54].
443 The reporter vector pHAGE-N CMVt N-RIG3 p53(R273C) (p7709), which contains a variant
444 of the GPS reporter cassette, expresses p53(R273C) fused to the monomeric red
445 fluorescent protein mRuby and a monomeric green fluorescent protein (SGFP2) fused to a
446 histone 2B (H2BC11) as reference (Fig 1A) [18]. The vectors pGL4.20-HPV16-LCR-
447 luciferase (p6239) and pGL4.20-HPV18-LCR-luciferase (p5194), expressing the firefly
448 luciferase under the control of the HPV16 and HPV18 LCRs respectively, have been

449 previously described [55]. Renilla luciferase was amplified from pRL-TK-Rluc (Promega #
450 E2241 - GenBank® Accession Number AF025846) using the primers 5'-
451 CAAGTCGACATGACTTCGAAAGTTTAT-3' and 5'-CTTAAGCTTATTGTTCATTTTTGAGAA-3',
452 and cloned into the p1318 human β-actin-based mammalian expression plasmid, which
453 contains a 4.3-kilobase EcoRI-AluI human β-actin promoter fragment, the human β-actin 3'
454 untranslated region, poly(A) site, and 3' flanking region [20] to generate (p7988).

455 **Cell lines**

456 HeLa, HeLa GPS p53(R273C), HeLa RIG3 p53(R273C), Siha (ATCC® HTB-35™), C33A
457 (ATCC® HTB-31™), U2OS (ATCC® HTB-96™), ME-180 (ATCC® HTB-33™), MS-751
458 (ATCC® HTB-34™), and human keratinocytes immortalized by HPV16 E6 and E7 expressed
459 from the β-actin promoter (p1321) [20] refered to here as 1321 cells were grown in
460 Dulbecco's modified Eagle's medium (DMEM) supplemented with 10% (v/v) fetal bovine
461 serum at 37°C 5% CO2.

462 **miRNA screen**

463 For the primary miRNA screen, HeLa GPS p53(R273C) cells were reverse transfected with
464 the Ambion Human Pre-miR miRNA Mimic Library (2009) based on miRBase release 13.0.
465 in a one-target, one-well format using 384-well microtiter plates in a high-throughput
466 format. The Z'-factor [56] was calculated for each assay plate and was consistently > 0.6,
467 indicating assay robustness. siRNA buffer (1×) (Horizon #B-002000-UB-100) was
468 aliquoted into wells, miRNA mimics were added so that the final concentration was 40
469 nM/well, and DharmaFECT1/OptiMEM was dispensed into wells. While the miRNA/lipid
470 mix was allowed to complex, cells were trypsinized, counted, and resuspended to reach a

471 plating density of 600 cells/well. Cells were seeded on top of the miRNA/lipid mixture,
472 briefly centrifuged, and incubated for 72 hours, a time that we determined to be optimal for
473 p53 stabilization for small miRNAs. The cells were then equilibrated to room temperature
474 (~15 min) before analysis. Using TTP LabTech's Acumen eX3 laser scanning cytometer, the
475 total EGFP and DsRed intensities in each well were quantitated. Internal controls were
476 present in Columns 13 and 14 of each library plate (Pre-miR miRNA Precursor Molecules
477 Negative Control #1 - Ambion AM17110; Pre-miR miRNA Precursor Molecules Negative
478 Control #2 – Ambion AM17111; PLK1 SMARTpool Dharmacon M-003290-01). In addition,
479 siRNAs against E6AP (UBE3A, Dharmacon D-005137-04) and non-targeting siRNAs
480 (Dharmacon D-001210-01 and D-001210-02) were added to each plate. The miRNA
481 mimics were screened in triplicate. High-throughput libraries and screening capability was
482 provided by the ICCB-Longwood Screening Facility at Harvard Medical School.

483 miRNA transfections

484 All cells were reverse transfected with miRNAs (S2 Table) using RNAiMax according to
485 manufacturer's instructions (ThermoFisher Scientific). More specifically, 750 µl of
486 suspended cells were added to 250 µl of a transfection mix containing 2 µl of Lipofectamine
487 RNAiMax and different miRNAs for a final concentration of 10nM and plated in 12-well
488 plates. miRNA transfection efficiency in different cell lines was confirmed using siGlo Red
489 Transfection Indicator (Horizon, D-001630-02-05).

490 Confirmation assay

491 HeLa cells were reverse transfected with 10 nM of the indicated miRNAs using
492 Lipofectamine RNAiMAX according to manufacturer's instructions. 72h after transfection

493 the cells were trypsinized, harvested in 1X flow cytometry buffer (1X PBS, 1mM EDTA, 2%
494 FBS) and analyzed for green and red fluorescence by flow cytometry using a BD
495 FACSymphony instrument (BD-Biosciences).

496 Western blots and antibodies

497 After incubation for 72h, transfected cells were washed once with 1X PBS, lysed directly in
498 wells with 100-150µl of SDS Lysis buffer (62.5mM Tris-Cl, pH 6.8, 2% SDS) and sonicated
499 (amplitude of 35%; 10 pulses with 2 seconds ON and 0.5 seconds OFF). The lysates were
500 centrifuged for 2 minutes and protein concentrations quantitated by BCA Protein Assay
501 (Pierce). Lysates (10 µg of protein/well) were run on 20-well 10-20% NuPage BisTris midi
502 gels in 1X MES buffer (ThermoFisher Scientific) and transferred to polyvinylidene
503 difluoride (PVDF) membranes using 25 mM Tris-HCl pH 7.6, 192 mM glycine, and 10%
504 methanol. Membranes were blocked in 5% nonfat dried milk in Tris-buffered saline [pH
505 7.4], 0.05% Tween 20 (TBST) and then incubated with primary antibodies as follows:
506 mouse monoclonal anti-E6AP (clone E4) at 1:1000 dilution (sc-166689 from Santa Cruz
507 Biotechnology); rabbit monoclonal anti-cleaved PARP (Asp214) (D64E10 XP® #5625 from
508 Cell Signaling Technologies); mouse monoclonal anti-HPV18-E6 (clone G-7) at a 1:250
509 dilution (sc-365089 from Santa Cruz Biotechnology); and mouse monoclonal anti-HPV18-
510 E7 (clone F-7) at a 1:250 dilution (sc-365035 from Santa Cruz Biotechnology). Membranes
511 were washed in TBST and incubated with horseradish peroxidase (HRP)-conjugated anti-
512 mouse antibody at a 1:1,000 dilution (R1005 from Kindle Biosciences). The primary
513 antibodies against β-Actin and P53 were directly conjugated to HRP and were used as
514 follows: mouse monoclonal anti-β-Actin-HRP at a 1:50,000 dilution (A3854 from Millipore
515 Sigma); and goat polyclonal anti-p53-HRP at a 1:3,000 dilution (HAF1355 from R&D

516 systems). All blots were developed using KwikQuant Ultra Digital-ECL™ Substrate Solution
517 and processed using KwikQuant™ Imager (Kindle Bioscience LLC). Western blots were
518 quantified using the Image Studio Lite program (LI-COR Biotechnologies).

519 RNA isolation and qRT-PCR.

520 At 72h post-transfection, total RNA was isolated using the Nucleospin RNA kit (Takara Bio)
521 according to the manufacturer's instructions. Samples were quantified using NanoDrop™
522 Lite Spectrophotometer and equal amounts of RNA (500ng) were reverse transcribed using
523 the high-capacity cDNA reverse transcription kit (Applied Biosystems). Quantitative real-
524 time PCR (qRT-PCR) was performed in an Applied Biosystems ABI 7500 fast sequence
525 detection system using TaqMan Fast Advanced Master Mix (ThermoFisher Scientific), and
526 the following TaqMan custom gene expression assays for HPV18-E6E7: HPV18-E6E7 FWD
527 5'-CAACCGAGCACGACAGGAA-3'; HPV18-E6E7 PROBE 5'-
528 AATATTAAGTATGCATGGACCTAAGGCAACATTGCAA-3'; and HPV18-E6E7 REV 5'-
529 CTCGTCGGGCTGGTAAATGTT-3' and for HPV16-E6E7: HPV16-E6-FWD 5'-
530 AGGAGCGACCCGGAAAGT-3'; HPV16-E6-PROBE 5'-
531 ACCACAGTTATGCACAGAGCTGCAAACAA-3'; and HPV16-E6-REV 5'-
532 CACGTCGCAGTAACTGTTGCTT-3'. All reactions were normalized using a TaqMan gene
533 expression assay for PPIA (Hs99999904_m1 ThermoFisher Scientific).

534 Luciferase assays

535 C33A cells were transfected in 12-well plates with 10 nM of miRNAs as described above.
536 After 24h, the miRNA transfection mix was removed and cells were transfected with 0.5 µg
537 of either plasmid pGL4-LCRHPV16 (p6239, HPV16 nt 7000-85) [55] or pGL4-LCRHPV18

538 (p5194, HPV18 nt 6943-105) [57], containing the firefly luciferase ORF under the control of
539 the HPV16 and HPV18 LCRs respectively, together with 0.5µg of a plasmid expressing the
540 renilla luciferase under the control of the human β-actin promoter using Lipofectamine
541 3000 (ThermoFisher Scientific) according to manufacturer's protocol. At 48h post-
542 transfection of plasmids (72 hours after miRNA transfection), cells were lysed in the plate
543 with 250 µl of 1x Passive Lysis Buffer and luciferase activity was determined using the
544 Dual-Luciferase Reporter Assay System (Promega) according to the manufacturer's
545 instructions. Luciferase intensities were measured using a SpectraMax L luminescence
546 microplate reader (Molecular Devices). Firefly luciferase readings were normalized to the
547 respective renilla luciferase readings.

548 **Apoptosis assays**

549 HeLa cells were reverse transfected with 10 nM of the different miRNAs either alone or
550 combined with 20 nM of siRNAs directed to p53 (Dharmacon, D-003329-26: 5'-
551 GCUUCGAGAUGUUCCGAGA-3') or its C911 version (sense, 5'-GCUUCGAGUACUUCCGAGA-
552 UU-3') using Lipofectamine RNAiMAX according to manufacturer's instructions. After
553 incubation for 72h, attached cells were trypsinized and combined with all non-adherent
554 cells in the supernatant and PBS washes. The cells were stained with Annexin V using the
555 Dead Cell Apoptosis Kit with Annexin V Alexa Fluor™ 488 & Propidium Iodide (PI)
556 (ThermoFisher Scientific #V13241 and #V13245). Stained cells were analyzed by flow
557 cytometry using a BD FACSCanto flow cytometer (BD Biosciences).

558 **Figures and statistics**

559 All graphics and statistical analyses were conducted using Prism 8 (GraphPad). When the
560 values corresponding to mock transfections were used to normalize other values obtained
561 in an experiment, the mock values were not included in the corresponding graphic since
562 invariably their mean is equal to one and their standard deviation is zero. Figures were
563 assembled using Affinity Photo (Affinity).

564 Acknowledgements

565 We thank other members of the Howley laboratory for helpful discussions and suggestions.
566 All plasmids generated in the Howley laboratory that are described in this manuscript are
567 available through Addgene. This work has been supported by NIH grant R35CA197262 to
568 P.M.H.

569

570 Bibliography

571 1. Howley PM, Schiller JT, Lowy DR. Papillomaviruses. In: Knipe DM, Howley PM,
572 editors. Fields Virology. 6th ed. Philadelphia: Lippincott, Williams and Wilkins; 2013. p.
573 1662-703.
574 2. de Martel C, Plummer M, Vignat J, Franceschi S. Worldwide burden of cancer
575 attributable to HPV by site, country and HPV type. Int J Cancer. 2017;141(4):664-70. Epub
576 2017/04/04. doi: 10.1002/ijc.30716. PubMed PMID: 28369882; PubMed Central PMCID:
577 PMCPMC5520228.
578 3. Goodwin EC, DiMaio D. Repression of human papillomavirus oncogenes in HeLa
579 cervical carcinoma cells causes the orderly reactivation of dormant tumor suppressor

580 pathways. Proc Natl Acad Sci U S A. 2000;97(23):12513-8. Epub 2000/11/09. doi:
581 10.1073/pnas.97.23.12513. PubMed PMID: 11070078; PubMed Central PMCID:
582 PMCPMC18795.
583 4. Wells SI, Francis DA, Karpova AY, Dowhanick JJ, Benson JD, Howley PM.
584 Papillomavirus E2 induces senescence in HPV positive cells via pRB- and $p21^{CIP}$-dependent
585 pathways. EMBO J. 2000;19:5762-71.
586 5. Scheffner M, Werness BA, Huibregtse JM, Levine AJ, Howley PM. The E6 oncoprotein
587 encoded by human papillomavirus types 16 and 18 promotes the degradation of p53. Cell.
588 1990;63(6):1129-36. Epub 1990/12/21. doi: 10.1016/0092-8674(90)90409-8. PubMed
589 PMID: 2175676.
590 6. Huibregtse JM, Scheffner M, Howley PM. Cloning and expression of the cDNA for E6-
591 AP: A protein that mediates the interaction of the human papillomavirus E6 oncoprotein
592 with p53. Mol Cell Biol. 1993;13:775-84.
593 7. Huibregtse JM, Scheffner M, Howley PM. Localization of the E6-AP regions that
594 direct HPV E6 binding, association with p53, and ubiquination of associated proteins. Mol
595 Cell Biol. 1993;13:4918-27.
596 8. Scheffner M, Huibregtse JM, Vierstra RD, Howley PM. The HPV-16 E6 and E6-AP
597 complex functions as a ubiquitin-protein ligase in the ubiquination of p53. Cell.
598 1993;75:495-505.
599 9. Park RB, Androphy EJ. Genetic analysis of high-risk e6 in episomal maintenance of
600 human papillomavirus genomes in primary human keratinocytes. J Virol.
601 2002;76(22):11359-64. PubMed PMID: 12388696.

602 10. Butz K, Ristriani T, Hengstermann A, Denk C, Scheffner M, Hoppe-Seyler F. siRNA
603 targeting of the viral E6 oncogene efficiently kills human papillomavirus-positive cancer
604 cells. Oncogene. 2003;22:5938-3945. doi: 10.1038/sj.onc.1206894
605 1206894 [pii]. PubMed PMID: 12955072.
606 11. Chirayil R, Kincaid RP, Dahlke C, Kuny CV, Dalken N, Spohn M, et al. Identification of
607 virus-encoded microRNAs in divergent Papillomaviruses. PLoS Pathog.
608 2018;14(7):e1007156. Epub 2018/07/27. doi: 10.1371/journal.ppat.1007156. PubMed
609 PMID: 30048533; PubMed Central PMCID: PMCPMC6062147.
610 12. Wald AI, Hoskins EE, Wells SI, Ferris RL, Khan SA. Alteration of microRNA profiles in
611 squamous cell carcinoma of the head and neck cell lines by human papillomavirus. Head
612 Neck. 2011;33(4):504-12. Epub 2010/07/24. doi: 10.1002/hed.21475. PubMed PMID:
613 20652977; PubMed Central PMCID: PMCPMC3080748.
614 13. Wang X, Wang HK, Li Y, Hafner M, Banerjee NS, Tang S, et al. microRNAs are
615 biomarkers of oncogenic human papillomavirus infections. Proc Natl Acad Sci U S A.
616 2014;111(11):4262-7. Epub 2014/03/05. doi: 10.1073/pnas.1401430111. PubMed PMID:
617 24591631; PubMed Central PMCID: PMCPMC3964092.
618 14. Tornesello ML, Faraonio R, Buonaguro L, Annunziata C, Starita N, Cerasuolo A, et al.
619 The Role of microRNAs, Long Non-coding RNAs, and Circular RNAs in Cervical Cancer.
620 Front Oncol. 2020;10:150. Epub 2020/03/11. doi: 10.3389/fonc.2020.00150. PubMed
621 PMID: 32154165; PubMed Central PMCID: PMCPMC7044410.
622 15. Scheffner M, Takahashi T, Huibregtse JM, Minna JD, Howley PM. Interaction of the
623 human papillomavirus type 16 E6 oncoprotein with wild-type and mutant human p53

624 proteins. J Virol. 1992;66(8):5100-5. Epub 1992/08/01. PubMed PMID: 1321290; PubMed
625 Central PMCID: PMCPMC241378.
626 16. Hubbert NL, Sedman SA, Schiller JT. Human papillomavirus type 16 E6 increases the
627 degradation rate of p53 in human keratinocytes. Journal of virology. 1992;66(10):6237-41.
628 PubMed PMID: 1326671.
629 17. Jung HM, Phillips BL, Chan EK. miR-375 activates p21 and suppresses telomerase
630 activity by coordinately regulating HPV E6/E7, E6AP, CIP2A, and 14-3-3zeta. Mol Cancer.
631 2014;13:80. Epub 2014/04/09. doi: 10.1186/1476-4598-13-80. PubMed PMID: 24708873;
632 PubMed Central PMCID: PMCPMC4021670.
633 18. Kuhnle S, Martinez-Noel G, Leclere F, Hayes SD, Harper JW, Howley PM. Angelman
634 syndrome-associated point mutations in the Zn(2+)-binding N-terminal (AZUL) domain of
635 UBE3A ubiquitin ligase inhibit binding to the proteasome. J Biol Chem.
636 2018;293(47):18387-99. Epub 2018/09/28. doi: 10.1074/jbc.RA118.004653. PubMed
637 PMID: 30257870; PubMed Central PMCID: PMCPMC6254356.
638 19. Scheffner M, Munger K, Byrne JC, Howley PM. The state of the p53 and
639 retinoblastoma genes in human cervical carcinoma cell lines. Proc Natl Acad Sci U S A.
640 1991;88(13):5523-7. Epub 1991/07/01. doi: 10.1073/pnas.88.13.5523. PubMed PMID:
641 1648218; PubMed Central PMCID: PMCPMC51909.
642 20. Munger K, Phelps WC, Bubb V, Howley PM, Schlegel R. The E6 and E7 genes of the
643 human papillomavirus type 16 together are necessary and sufficient for transformation of
644 primary human keratinocytes. J Virol. 1989;63(10):4417-21. Epub 1989/10/01. PubMed
645 PMID: 2476573; PubMed Central PMCID: PMCPMC251060.

646 21. Liu X. Up-regulation of miR-20a by HPV16 E6 exerts growth-promoting effects by
647 targeting PDCD6 in cervical carcinoma cells. Biomed Pharmacother. 2018;102:996-1002.
648 Epub 2018/05/02. doi: 10.1016/j.biopha.2018.03.154. PubMed PMID: 29710555.
649 22. Buehler E, Chen YC, Martin S. C911: A bench-level control for sequence specific
650 siRNA off-target effects. PLoS One. 2012;7(12):e51942. Epub 2012/12/20. doi:
651 10.1371/journal.pone.0051942. PubMed PMID: 23251657; PubMed Central PMCID:
652 PMCPMC3522603.
653 23. Jiang Y, Hou R, Li S, Li S, Dang G. MicroRNA-302 inhibits cell migration and invasion
654 in cervical cancer by targeting DCUN1D1. Exp Ther Med. 2018;16(2):1000-8. Epub
655 2018/08/18. doi: 10.3892/etm.2018.6223. PubMed PMID: 30116351; PubMed Central
656 PMCID: PMCPMC6090382.
657 24. Li GC, Cao XY, Li YN, Qiu YY, Li YN, Liu XJ, et al. MicroRNA-374b inhibits cervical
658 cancer cell proliferation and induces apoptosis through the p38/ERK signaling pathway by
659 binding to JAM-2. J Cell Physiol. 2018;233(9):7379-90. Epub 2018/03/27. doi:
660 10.1002/jcp.26574. PubMed PMID: 29575013.
661 25. Mou Z, Xu X, Dong M, Xu J. MicroRNA-148b Acts as a Tumor Suppressor in Cervical
662 Cancer by Inducing G1/S-Phase Cell Cycle Arrest and Apoptosis in a Caspase-3-Dependent
663 Manner. Med Sci Monit. 2016;22:2809-15. Epub 2016/08/10. doi: 10.12659/msm.896862.
664 PubMed PMID: 27505047; PubMed Central PMCID: PMCPMC4982527.
665 26. Ji F, Du R, Chen T, Zhang M, Zhu Y, Luo X, et al. Circular RNA circSLC26A4
666 Accelerates Cervical Cancer Progression via miR-1287-5p/HOXA7 Axis. Mol Ther Nucleic
667 Acids. 2020;19:413-20. Epub 2020/01/03. doi: 10.1016/j.omtn.2019.11.032. PubMed
668 PMID: 31896069; PubMed Central PMCID: PMCPMC6940609.

669 27. Abdelmohsen K, Kim MM, Srikantan S, Mercken EM, Brennan SE, Wilson GM, et al.
670 miR-519 suppresses tumor growth by reducing HuR levels. Cell Cycle. 2010;9(7):1354-9.
671 Epub 2010/03/23. doi: 10.4161/cc.9.7.11164. PubMed PMID: 20305372; PubMed Central
672 PMCID: PMCPMC3057889.
673 28. Abdelmohsen K, Srikantan S, Tominaga K, Kang MJ, Yaniv Y, Martindale JL, et al.
674 Growth inhibition by miR-519 via multiple p21-inducing pathways. Mol Cell Biol.
675 2012;32(13):2530-48. Epub 2012/05/02. doi: 10.1128/mcb.00510-12. PubMed PMID:
676 22547681; PubMed Central PMCID: PMCPMC3434494.
677 29. Chen Y, Wang X. miRDB: an online database for prediction of functional microRNA
678 targets. Nucleic Acids Res. 2020;48(D1):D127-D31. Epub 2019/09/11. doi:
679 10.1093/nar/gkz757. PubMed PMID: 31504780; PubMed Central PMCID:
680 PMCPMC6943051.
681 30. Liu W, Wang X. Prediction of functional microRNA targets by integrative modeling of
682 microRNA binding and target expression data. Genome Biol. 2019;20(1):18. Epub
683 2019/01/24. doi: 10.1186/s13059-019-1629-z. PubMed PMID: 30670076; PubMed
684 Central PMCID: PMCPMC6341724.
685 31. Kim JY, Kim KM, Yang JH, Cho SS, Kim SJ, Park SJ, et al. Induction of E6AP by
686 microRNA-302c dysregulation inhibits TGF-beta-dependent fibrogenesis in hepatic stellate
687 cells. Sci Rep. 2020;10(1):444. Epub 2020/01/18. doi: 10.1038/s41598-019-57322-w.
688 PubMed PMID: 31949242; PubMed Central PMCID: PMCPMC6965100.
689 32. Kedde M, Strasser MJ, Boldajipour B, Oude Vrielink JA, Slanchev K, le Sage C, et al.
690 RNA-binding protein Dnd1 inhibits microRNA access to target mRNA. Cell.

691 2007;131(7):1273-86. Epub 2007/12/25. doi: 10.1016/j.cell.2007.11.034. PubMed PMID:
692 18155131.
693 33. Mockly S, Seitz H. Inconsistencies and Limitations of Current MicroRNA Target
694 Identification Methods. Methods Mol Biol. 2019;1970:291-314. Epub 2019/04/10. doi:
695 10.1007/978-1-4939-9207-2_16. PubMed PMID: 30963499.
696 34. Girardi E, Lopez P, Pfeffer S. On the Importance of Host MicroRNAs During Viral
697 Infection. Front Genet. 2018;9:439. Epub 2018/10/20. doi: 10.3389/fgene.2018.00439.
698 PubMed PMID: 30333857; PubMed Central PMCID: PMCPMC6176045.
699 35. Wang F, Li Y, Zhou J, Xu J, Peng C, Ye F, et al. miR-375 is down-regulated in
700 squamous cervical cancer and inhibits cell migration and invasion via targeting
701 transcription factor SP1. Am J Pathol. 2011;179(5):2580-8. Epub 2011/09/29. doi:
702 10.1016/j.ajpath.2011.07.037. PubMed PMID: 21945323; PubMed Central PMCID:
703 PMCPMC3204087.
704 36. Hoppe-Seyler F, Butz K. Activation of human papillomavirus type 18 E6-E7
705 oncogene expression by transcription factor Sp1. Nucleic Acids Res. 1992;20(24):6701-6.
706 Epub 1992/12/25. doi: 10.1093/nar/20.24.6701. PubMed PMID: 1336181; PubMed
707 Central PMCID: PMCPMC334589.
708 37. Tan SH, Leong LE, Walker PA, Bernard HU. The human papillomavirus type 16 E2
709 transcription factor binds with low cooperativity to two flanking sites and represses the E6
710 promoter through displacement of Sp1 and TFIID. J Virol. 1994;68(10):6411-20. Epub
711 1994/10/01. PubMed PMID: 8083979; PubMed Central PMCID: PMCPMC237061.
712 38. Hong L, Ya-Wei L, Hai W, Qiang Z, Jun-Jie L, Huang A, et al. MiR-519a functions as a
713 tumor suppressor in glioma by targeting the oncogenic STAT3 pathway. J Neurooncol.

714 2016;128(1):35-45. Epub 2016/03/14. doi: 10.1007/s11060-016-2095-z. PubMed PMID:
715 26970980.
716 39. Deng X, Zhao Y, Wang B. miR-519d-mediated downregulation of STAT3 suppresses
717 breast cancer progression. Oncol Rep. 2015;34(4):2188-94. Epub 2015/08/05. doi:
718 10.3892/or.2015.4160. PubMed PMID: 26238950.
719 40. Morgan EL, Wasson CW, Hanson L, Kealy D, Pentland I, McGuire V, et al. STAT3
720 activation by E6 is essential for the differentiation-dependent HPV18 life cycle. PLoS
721 Pathog. 2018;14(4):e1006975. Epub 2018/04/10. doi: 10.1371/journal.ppat.1006975.
722 PubMed PMID: 29630659; PubMed Central PMCID: PMCPMC5908086.
723 41. Shukla S, Mahata S, Shishodia G, Pandey A, Tyagi A, Vishnoi K, et al. Functional
724 regulatory role of STAT3 in HPV16-mediated cervical carcinogenesis. PLoS One.
725 2013;8(7):e67849. Epub 2013/07/23. doi: 10.1371/journal.pone.0067849. PubMed PMID:
726 23874455; PubMed Central PMCID: PMCPMC3715508.
727 42. Xun Y, Tang Y, Hu L, Xiao H, Long S, Gong M, et al. Purification and Identification of
728 miRNA Target Sites in Genome Using DNA Affinity Precipitation. Front Genet. 2019;10:778.
729 Epub 2019/10/02. doi: 10.3389/fgene.2019.00778. PubMed PMID: 31572429; PubMed
730 Central PMCID: PMCPMC6751328.
731 43. Kracikova M, Akiri G, George A, Sachidanandam R, Aaronson SA. A threshold
732 mechanism mediates p53 cell fate decision between growth arrest and apoptosis. Cell
733 Death Differ. 2013;20(4):576-88. Epub 2013/01/12. doi: 10.1038/cdd.2012.155. PubMed
734 PMID: 23306555; PubMed Central PMCID: PMCPMC3595483.

735 44. Bartel DP. MicroRNAs: target recognition and regulatory functions. Cell.
736 2009;136(2):215-33. Epub 2009/01/27. doi: 10.1016/j.cell.2009.01.002. PubMed PMID:
737 19167326; PubMed Central PMCID: PMCPMC3794896.
738 45. Shukla GC, Singh J, Barik S. MicroRNAs: Processing, Maturation, Target Recognition
739 and Regulatory Functions. Mol Cell Pharmacol. 2011;3(3):83-92. Epub 2011/01/01.
740 PubMed PMID: 22468167; PubMed Central PMCID: PMCPMC3315687.
741 46. Broughton JP, Lovci MT, Huang JL, Yeo GW, Pasquinelli AE. Pairing beyond the Seed
742 Supports MicroRNA Targeting Specificity. Mol Cell. 2016;64(2):320-33. Epub 2016/10/22.
743 doi: 10.1016/j.molcel.2016.09.004. PubMed PMID: 27720646; PubMed Central PMCID:
744 PMCPMC5074850.
745 47. Lee RC, Feinbaum RL, Ambros V. The C. elegans heterochronic gene lin-4 encodes
746 small RNAs with antisense complementarity to lin-14. Cell. 1993;75(5):843-54. Epub
747 1993/12/03. doi: 10.1016/0092-8674(93)90529-y. PubMed PMID: 8252621.
748 48. Wightman B, Ha I, Ruvkun G. Posttranscriptional regulation of the heterochronic
749 gene lin-14 by lin-4 mediates temporal pattern formation in C. elegans. Cell.
750 1993;75(5):855-62. Epub 1993/12/03. doi: 10.1016/0092-8674(93)90530-4. PubMed
751 PMID: 8252622.
752 49. Bonneau E, Neveu B, Kostantin E, Tsongalis GJ, De Guire V. How close are miRNAs
753 from clinical practice? A perspective on the diagnostic and therapeutic market. Ejifcc.
754 2019;30(2):114-27. Epub 2019/07/03. PubMed PMID: 31263388; PubMed Central PMCID:
755 PMCPMC6599191.
756 50. Hanna J, Hossain GS, Kocerha J. The Potential for microRNA Therapeutics and
757 Clinical Research. Front Genet. 2019;10:478. Epub 2019/06/04. doi:

758 10.3389/fgene.2019.00478. PubMed PMID: 31156715; PubMed Central PMCID:
759 PMCPMC6532434.
760 51. Emanuele MJ, Elia AE, Xu Q, Thoma CR, Izhar L, Leng Y, et al. Global identification of
761 modular cullin-RING ligase substrates. Cell. 2011;147(2):459-74. Epub 2011/10/04. doi:
762 10.1016/j.cell.2011.09.019. PubMed PMID: 21963094; PubMed Central PMCID:
763 PMCPMC3226719.
764 52. Lin HC, Yeh CW, Chen YF, Lee TT, Hsieh PY, Rusnac DV, et al. C-Terminal End-
765 Directed Protein Elimination by CRL2 Ubiquitin Ligases. Mol Cell. 2018;70(4):602-13 e3.
766 Epub 2018/05/19. doi: 10.1016/j.molcel.2018.04.006. PubMed PMID: 29775578; PubMed
767 Central PMCID: PMCPMC6145449.
768 53. Yen HC, Elledge SJ. Identification of SCF ubiquitin ligase substrates by global protein
769 stability profiling. Science. 2008;322(5903):923-9. Epub 2008/11/08. doi:
770 10.1126/science.1160462. PubMed PMID: 18988848.
771 54. Yen HC, Xu Q, Chou DM, Zhao Z, Elledge SJ. Global protein stability profiling in
772 mammalian cells. Science. 2008;322(5903):918-23. Epub 2008/11/08. doi:
773 10.1126/science.1160489. PubMed PMID: 18988847.
774 55. Ottinger M, Smith JA, Schweiger MR, Robbins D, Powell ML, You J, et al. Cell-type
775 specific transcriptional activities among different papillomavirus long control regions and
776 their regulation by E2. Virology. 2009;395(2):161-71. Epub 2009/10/20. doi:
777 10.1016/j.virol.2009.09.027. PubMed PMID: 19836046; PubMed Central PMCID:
778 PMCPMC2787971.
779 56. Zhang JH, Chung TD, Oldenburg KR. A Simple Statistical Parameter for Use in
780 Evaluation and Validation of High Throughput Screening Assays. J Biomol Screen.

781 1999;4(2):67-73. Epub 2000/06/06. doi: 10.1177/108705719900400206. PubMed PMID:
782 10838414.
783 57. Schweiger MR, Ottinger M, You J, Howley PM. Brd4-independent transcriptional
784 repression function of the papillomavirus e2 proteins. J Virol. 2007;81(18):9612-22. Epub
785 2007/07/13. doi: 10.1128/jvi.00447-07. PubMed PMID: 17626100; PubMed Central
786 PMCID: PMCPMC2045424.

787

788 # Figure captions

789

790 **Fig 1. Schematic representation of reporter cassettes.**
791 **A.** Reporter cassette of pHAGE-P CMVt RIG p53(R273C)**. B.** Reporter cassette in pHAGE-P
792 CMVt RIG3 p53(R273C). CMVp: CMV promoter, IRES: Encephalomyocarditis virus internal
793 ribosomal entry site, H2B: histone 2B (H2BC11), SG linker: serine-glycine linker.

794

795 **Fig 2. Effect of miRNAs transfection on p53, E6AP, and E6 protein levels in HeLa cells.**
796 Cells were lysed 72 h post-transfection and the lysates were resolved by SDS-PAGE. Protein
797 levels of p53, E6AP, E6, and actin were visualized by western blotting. **A, C, and E.** Western
798 blot results from a single experiment. **B, D, and F.** Quantification of p53 from western blot
799 experiments. Values obtained for p53 were normalized to the amount of actin in the same
800 sample and then all values were divided by the corresponding value obtained with the
801 mock transfection in the same blot. Circles represent values from independent experiments

802 and the bars show the mean ± standard deviation. To determine significant differences
803 between the samples in an experiment we used the “one-way ANOVA” test (A. $F(16, 34)=8.271$ $p<0.0001$, n=3; B. $F(14, 30)=17.76$ $p<0.0001$, n=3; C. $F(3, 12)=52.63$ $p<0.0001$,
805 n=4). We then compared each sample with the cells transfected with the Ctrl.1 miRNA
806 using the "Dunnett's multiple comparisons test" (* = $p<0.01$).
807
808 **Fig 3. Effect of transfection of selected miRNAs on p53 and E6AP protein levels in**
809 **different cell lines.**
810 72 h after transfection cells were lysed and the protein extracts were resolved by SDS-
811 PAGE, and the p53, E6AP, and actin proteins levels were determined by western blotting.
812
813 **Fig 4. Effect of selected miRNAs on HPV E6 and E7 expression.**
814 Cells were harvested 72 h post-transfection and then used for the following experiments. **A.**
815 Western blot showing the effect of the selected miRNAs on E6, E7, and actin protein levels
816 in HeLa cells. **B.** Effect of ectopic expression of selected miRNAs on the promoter activity of
817 the HPV16 and HPV18 LCRs using a luciferase reporter assay in C33A cells. Values from
818 each experiment were normalized to the value obtained for the corresponding mock
819 transfection. Differences between samples were analyzed by the “one-way ANOVA” test
820 (HPV 16 $F(12, 38) = 34.91$, n=4; HPV18 $F(12, 39) = 23.47$ $p<0.0001$, n=4), then each sample
821 was compared to the non-treated cells using the "Dunnett's multiple comparisons test" (* =
822 $p<0.01$). **C.** Expression of the E6/E7 mRNAs after transfection of the selected miRNAs was
823 quantitated by QRT-PCR. Measures from each experiment were normalized to the value of
824 the corresponding mock transfection. The same statistical analysis described in B. was

825 applied to these samples (SiHa $F(12, 26) = 41.38$ $p<0.0001$, n=3; HeLa $F(12, 39) = 42.32$
826 $p<0.0001$, n=4). In B. and C. Circles represent values from independent experiments and
827 the bars show the mean ± standard deviation.
828
829 **Fig 5. Ectopic miRNA expression induces apoptosis in HeLa cells.**
830 Cells were harvested 72 h post-transfection and stained with Annexin V as an indicator of
831 apoptosis. The percentage of cells stained with Annexin V was determined by flow
832 cytometry. Variability between samples was first analyzed with the one-way ANOVA test
833 ($F(12,26)=48.04$ $p<0.0001$, n=3). Then each sample was compared to the non-treated cells
834 with the "Dunnett's multiple comparisons test" (* = $p<0.01$). Circles represent values from
835 independent experiments and the bars show the mean ± standard deviation.
836
837 **Fig 6. Apoptotic effect of the selected miRNAs when transfected into different cell**
838 **lines.**
839 Cells were transfected with the indicated miRNAs and 72 h later the cells were harvested
840 and stained with Annexin V as a marker for apoptosis. The percentage of Annexin V
841 positive cells was quantitated by flow cytometry. Variability between samples for each cell
842 line was analyzed with the one-way ANOVA test (SiHa $F(6,21)=45.17$ $p<0.0001$, n=4; C33A
843 $F(6,21)=85.96$ $p<0.0001$, n=3; U2OS $F(6,21)=104.07$ $p<0.0001$, n=4). Each sample was then
844 compared to the non-treated cells with the "Dunnett's multiple comparisons test" (* =
845 $p<0.01$). Circles represent values from independent experiments and the bars show the
846 mean ± standard deviation.
847

848 **Fig 7. p53 dependence of apoptotic effect of selected miRNAs in HeLa cells. A.**
849 Cells were transfected with the indicated miRNAs either alone or together with a siRNA
850 against p53 or its C911 variant. After incubation for 72 h the cells were harvested and
851 stained with Annexin V as a marker for apoptosis. The percentage of Annexin V stained
852 cells was determined by flow cytometry. The values obtained for the three transfections
853 with each miRNA were first analyzed with the one-way ANOVA test (375-3p $F(2, 6) = 3.075$
854 $p=0.1204$; 498-5p $F(2, 6) = 1.914$ $p=0.2276$; 20a-3p $F(2, 6) = 0.6553$ $p=0.5528$; 148b-5p
855 $F(2, 6) = 23.57$ $p=0.0014$; 374a-3p $F(2, 6) = 2.681$ $p=0.1472$; 519b-3p $F(2, 6) = 17.71$
856 $p=0.0030$; 1287-5p $F(2, 6) = 48.00$ $p=0.0002$). For all samples n=3. Then, the values from
857 samples transfected with the same miRNA were compared with each other using the
858 "Tukey's multiple comparisons test" (* = $p<0.01$). **B.** 72 h post-transfection cells were lysed
859 and the p53, cleaved PARP, and GAPDH proteins levels were determined by SDS-PAGE and
860 western blotting.
861

862 # Supporting Information

863

864 **S1 Table. Screen data.**

865

866 **S1 Fig. Alignment of members of the 302/519 family of miRNAs.**
867 Several of the miRNAs identified in our screen have the same seed sequence indicated with
868 bold letters and underlined. [1] miRNAs with EGFP/DsRed ratios between top 50 positions in
869 the primary screen.

870

871 **S2 Fig. p53 stabilization in HeLa cells expressing the reporter pHAGE-P CMVt RIG3**

872 **p53(R273C).**

873 72 h after transfection cells were harvested and the percentage of cells expressing mRuby-

874 p53(R273C) was determined by flow cytometry. Columns indicate the means of three

875 independent experiments and the error bars show one standard deviation. Variability

876 between the means was tested using the one-way ANOVA test ($F(40, 82) = 84.19$

877 $p<0.0001$). Then, each sample was compared to non-treated cells using the "Dunnett's

878 multiple comparisons test" (* = $p<0.01$).

879

880 **S3 Fig. Quantification of the effect of miRNAs transfection on E6AP, and E6 protein**

881 **levels in HeLa cells.**

882 Quantification of E6AP and E6 protein levels from western blot experiments. The values for

883 E6AP and E6 were normalized to the amount of actin in the same sample, then all values

884 were divided by the corresponding value of the mock transfection in the same blot. Circles

885 show the values of independent experiments and the bars indicate the mean ± standard

886 deviation. The significance of differences between the samples means was determined

887 using the one-way ANOVA test (**A.** E6AP protein levels $F(16, 34)=9.540$ $p<0.0001$, n=3; **B.**

888 E6AP protein levels $F(14, 30)=1.218$ $p<0.3135$, n=3; **C.** E6AP protein levels $F(3, 12)=11.16$

889 $p<0.0009$, n=4 **D.** E6 protein levels $F(16, 34)=8.672$ $p<0.0001$, n=3; **E.** E6 protein levels

890 $F(14, 30)=18.15$ $p<0.0001$, n=3; **F.** E6 protein levels $F(3, 12)=55.35$ $p<0.0001$, n=4). Each

891 sample was then compared to the cells transfected with the Ctrl.1 miRNA using the

892 "Dunnett's multiple comparisons test" (* = $p<0.01$).

893

894 **S4 Fig. The protein levels of p53 negatively correlate with those of E6.**

895 The protein levels of p53, E6AP, and E6 calculated from the western blot experiments

896 displayed in Figs 2 and S3 were used to analyze whether there is a significant correlation

897 between the levels of these proteins after transfection of HeLa cells with the different

898 miRNAs. This was done by calculating the Pearson's correlation coefficient (r) and a two

899 tailed p value. **A.** Correlation between E6AP and p53. **B.** Correlation between E6 and p53. **C.**

900 Correlation between E6AP and E6.

901

902 **S2 Table. List of miRNAs used in this study.**

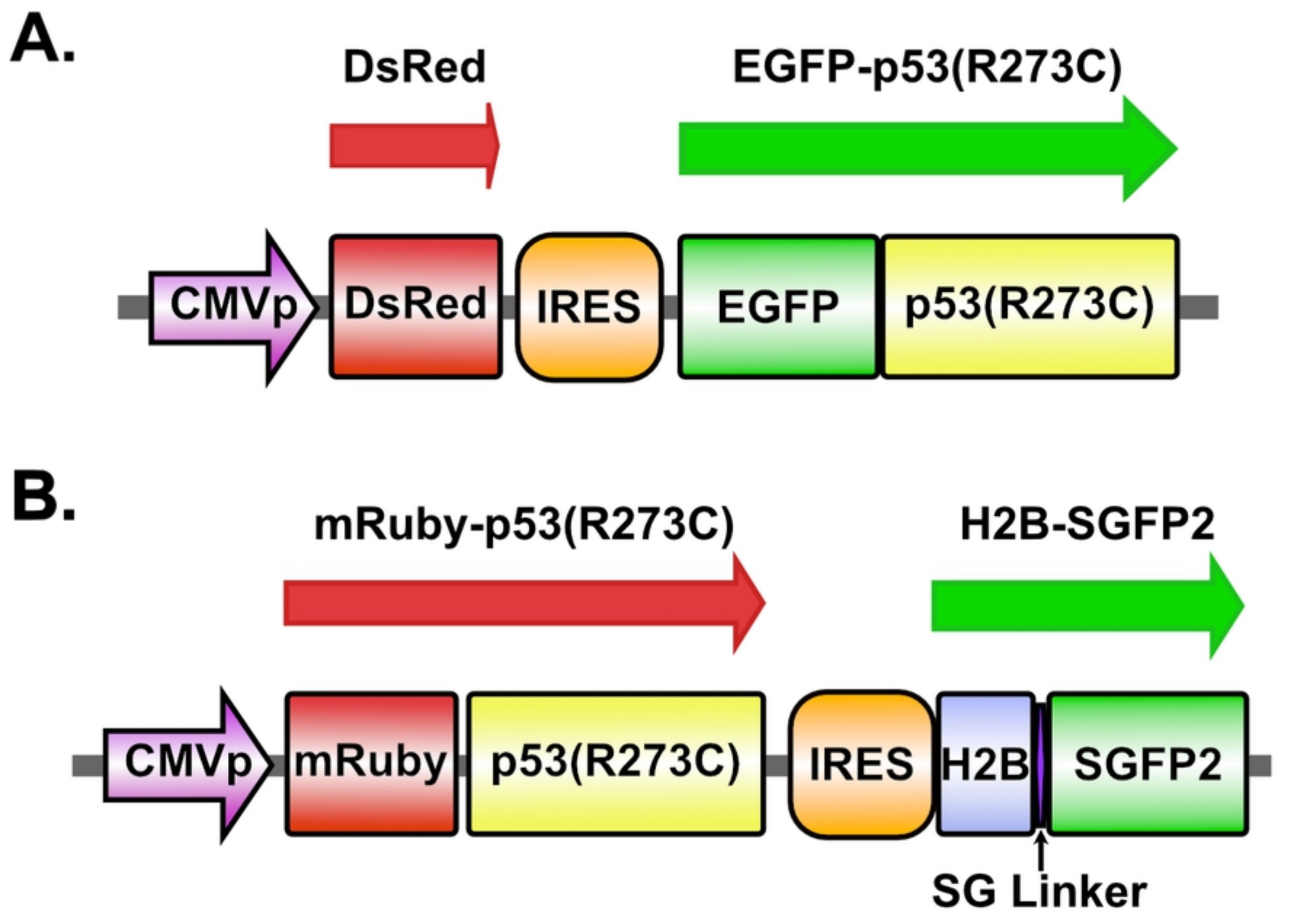
A.
DsRed
EGFP-p53(R273C)
CMVp
DsRed
IRES
EGFP
p53(R273C)
B.
mRuby-p53(R273C)
H2B-SGFP2
CMVp
mRuby
p53(R273C)
IRES
H2B
SGFP2
SG Linker

Figure 1

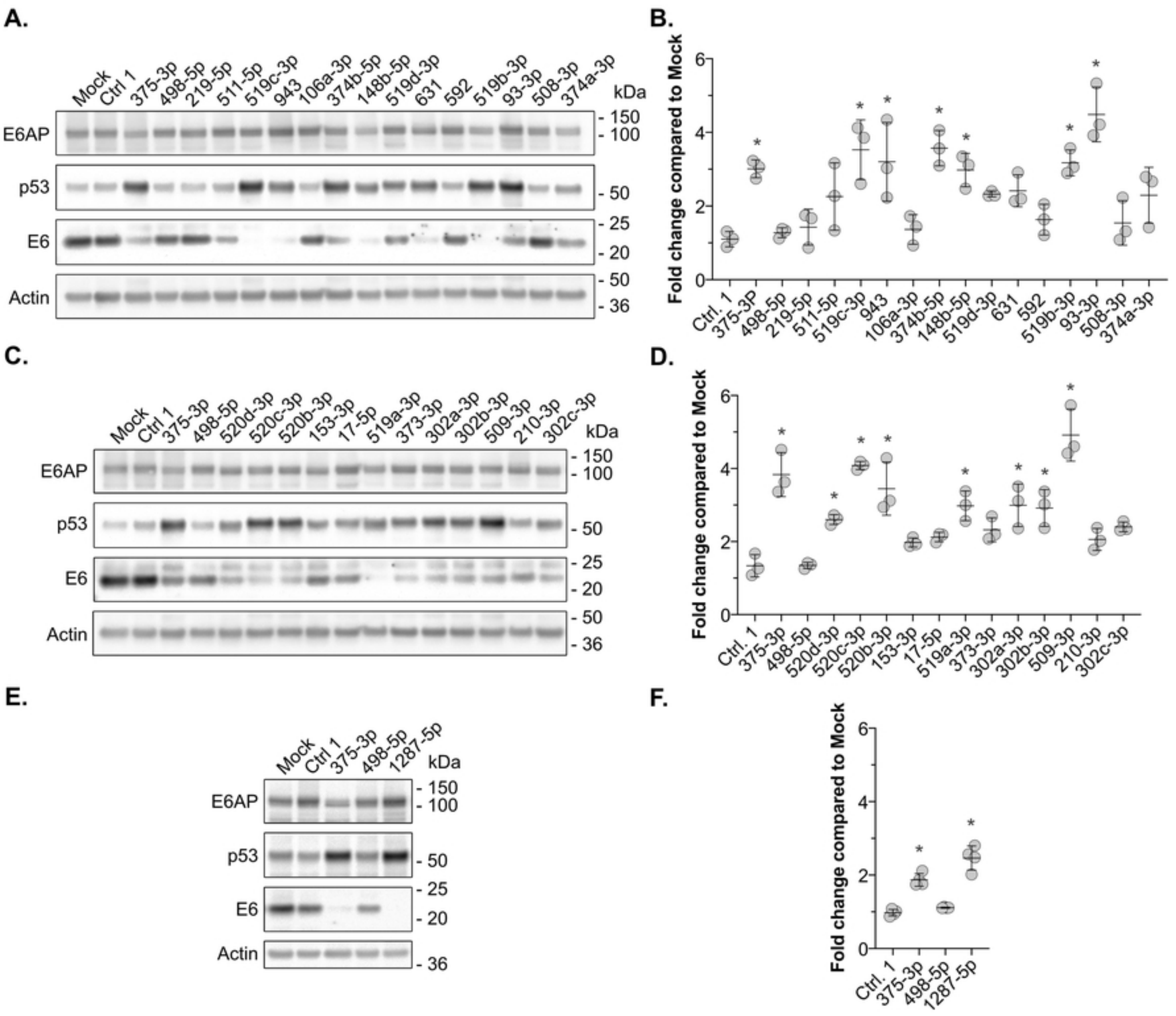
A.
Mock
Ctrl 1
375-3p
498-5p
219-5p
511-5p
519c-3p
943
106a-3p
374b-5p
148b-5p
519d-3p
631
592
519b-3p
93-3p
508-3p
374a-3p
kDa
E6AP
p53
E6
Actin
150
100
50
25
20
50
36
B.
Fold change compared to Mock
C.
520d-3p
520c-3p
520b-3p
153-3p
17-5p
519a-3p
373-3p
302a-3p
302b-3p
509-3p
210-3p
302c-3p
D.
E.
1287-5p
F.

Figure 2

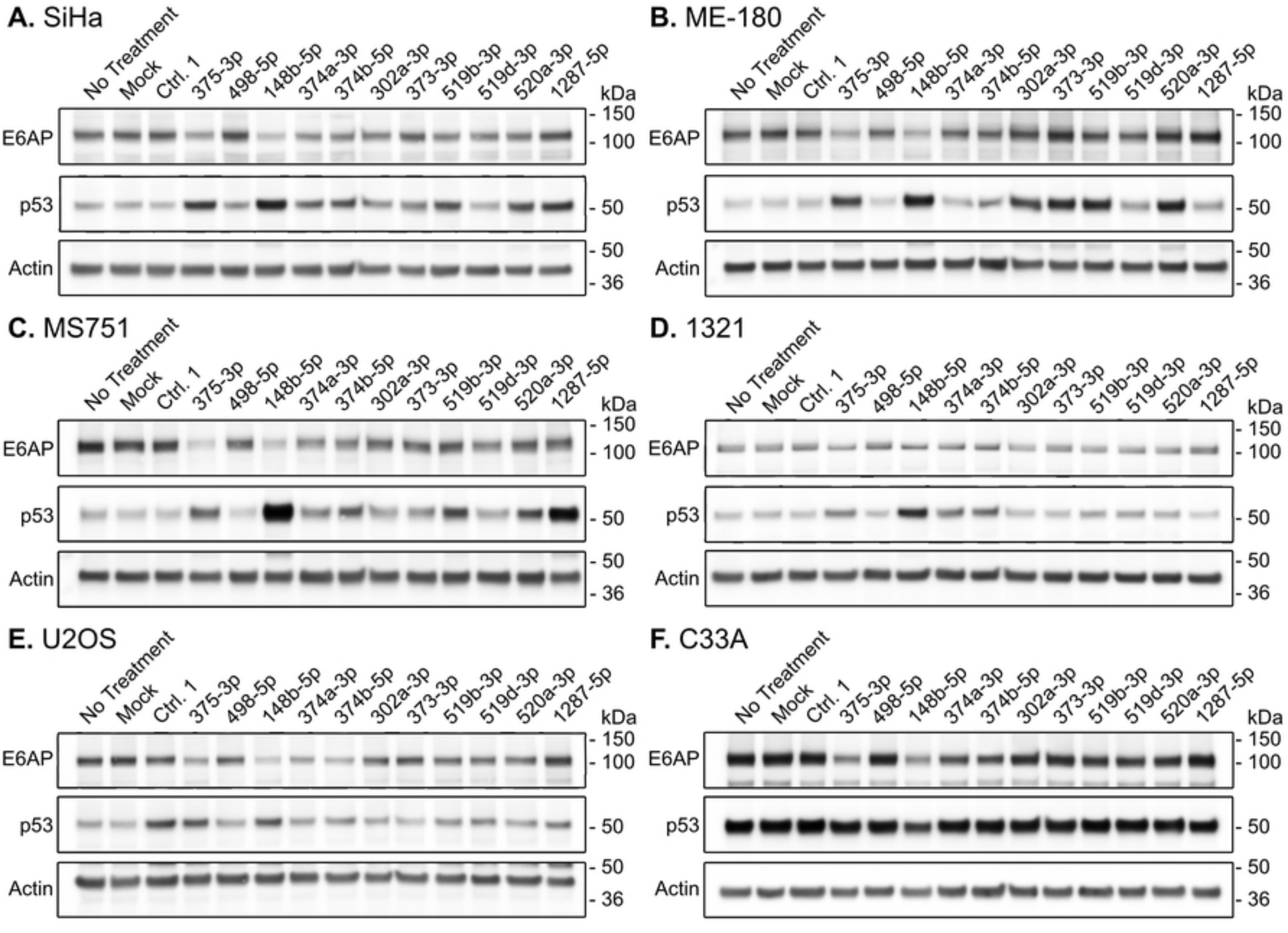
A. SiHa
B. ME-180
C. MS751
D. 1321
E. U2OS
F. C33A
No Treatment
Mock
Ctrl. 1
375-3p
498-5p
148b-5p
374a-3p
374b-5p
302a-3p
373-3p
519b-3p
519d-3p
520a-3p
1287-5p
kDa
E6AP
p53
Actin
150
100
50
50
36

Figure 3

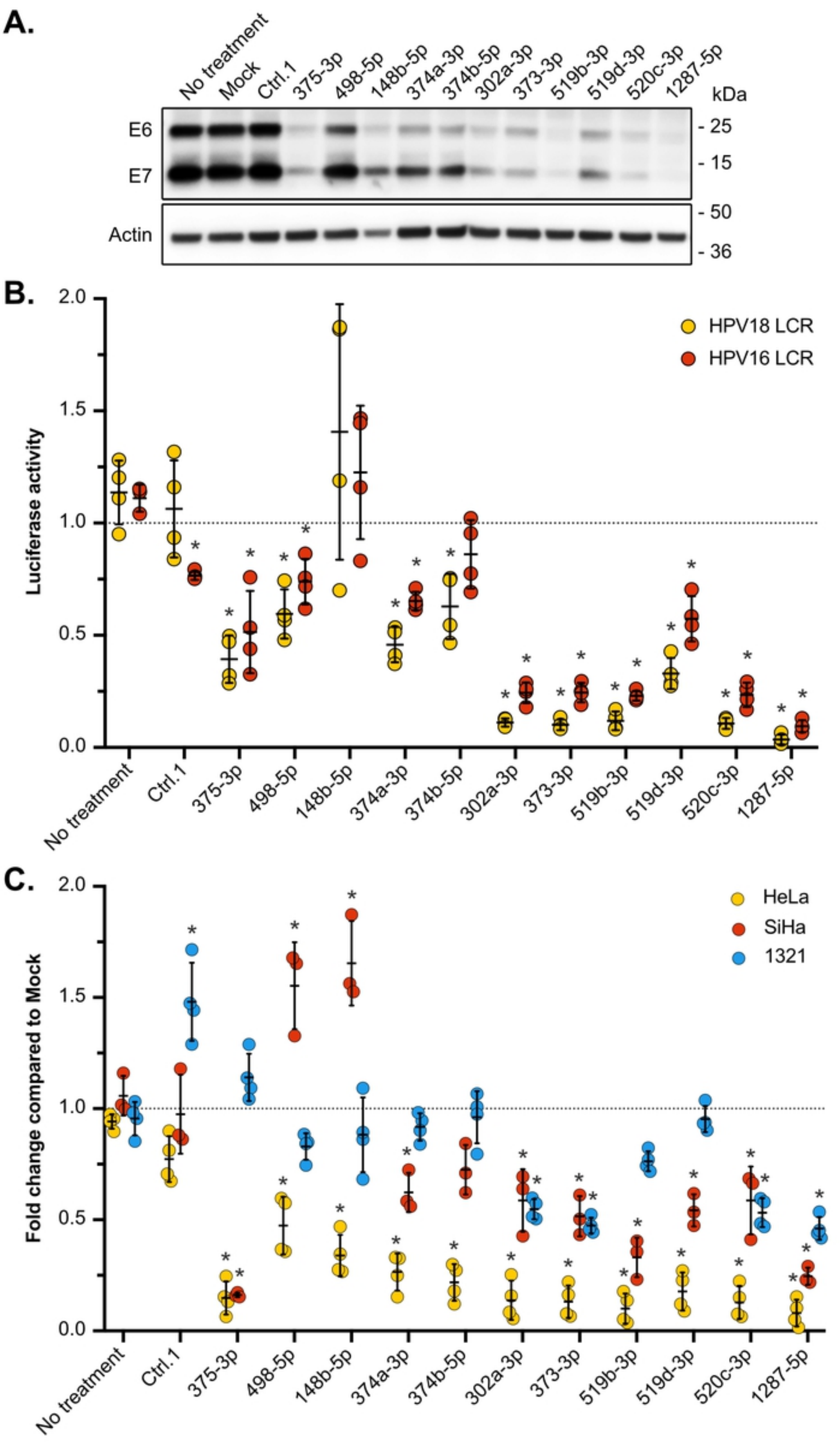
A.
No treatment
Mock
Ctrl.1
375-3p
498-5p
148b-5p
374a-3p
374b-5p
302a-3p
373-3p
519b-3p
519d-3p
520c-3p
1287-5p
kDa
E6
E7
Actin
- 25
- 15
- 50
- 36
B.
HPV18 LCR
HPV16 LCR
Luciferase activity
2.0
1.5
1.0
0.5
0.0
C.
HeLa
SiHa
1321
Fold change compared to Mock

Figure 4

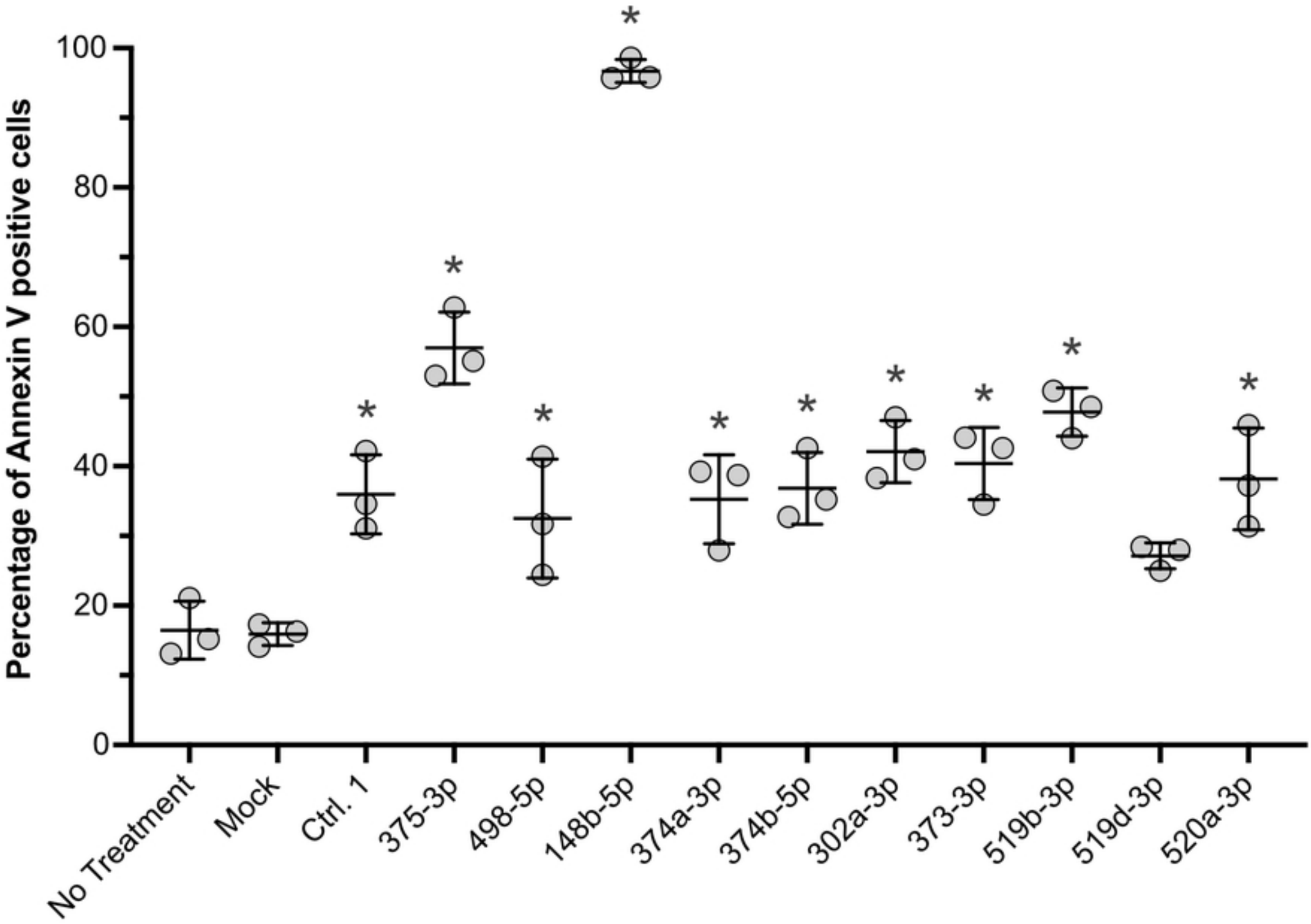
Percentage of Annexin V positive cells
100
80
60
40
20
0
No Treatment
Mock
Ctrl. 1
375-3p
498-5p
148b-5p
374a-3p
374b-5p
302a-3p
373-3p
519b-3p
519d-3p
520a-3p

Figure 5

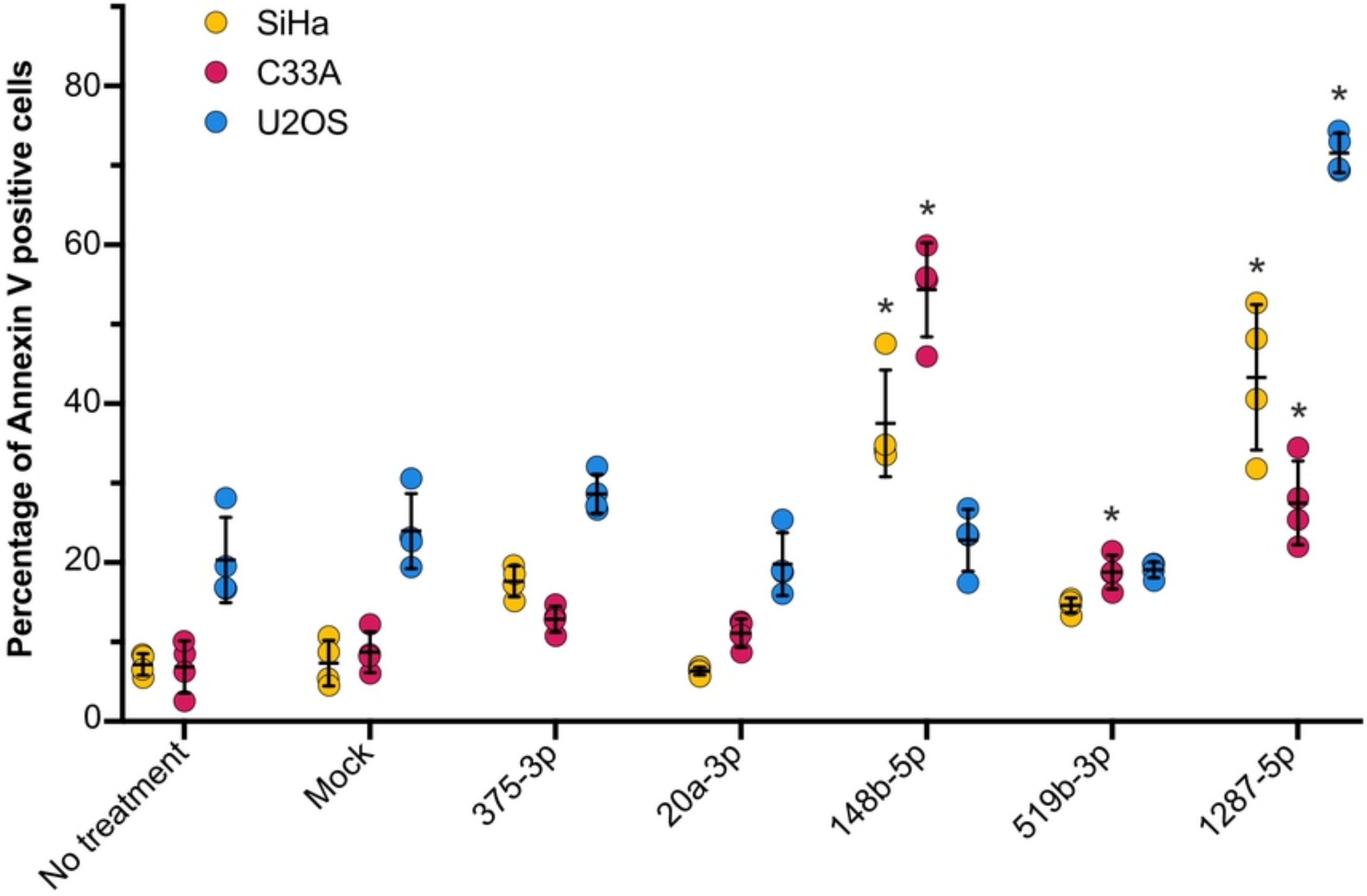
SiHa
C33A
U2OS
Percentage of Annexin V positive cells
0
20
40
60
80
*
No treatment
Mock
375-3p
20a-3p
148b-5p
519b-3p
1287-5p

Figure 6

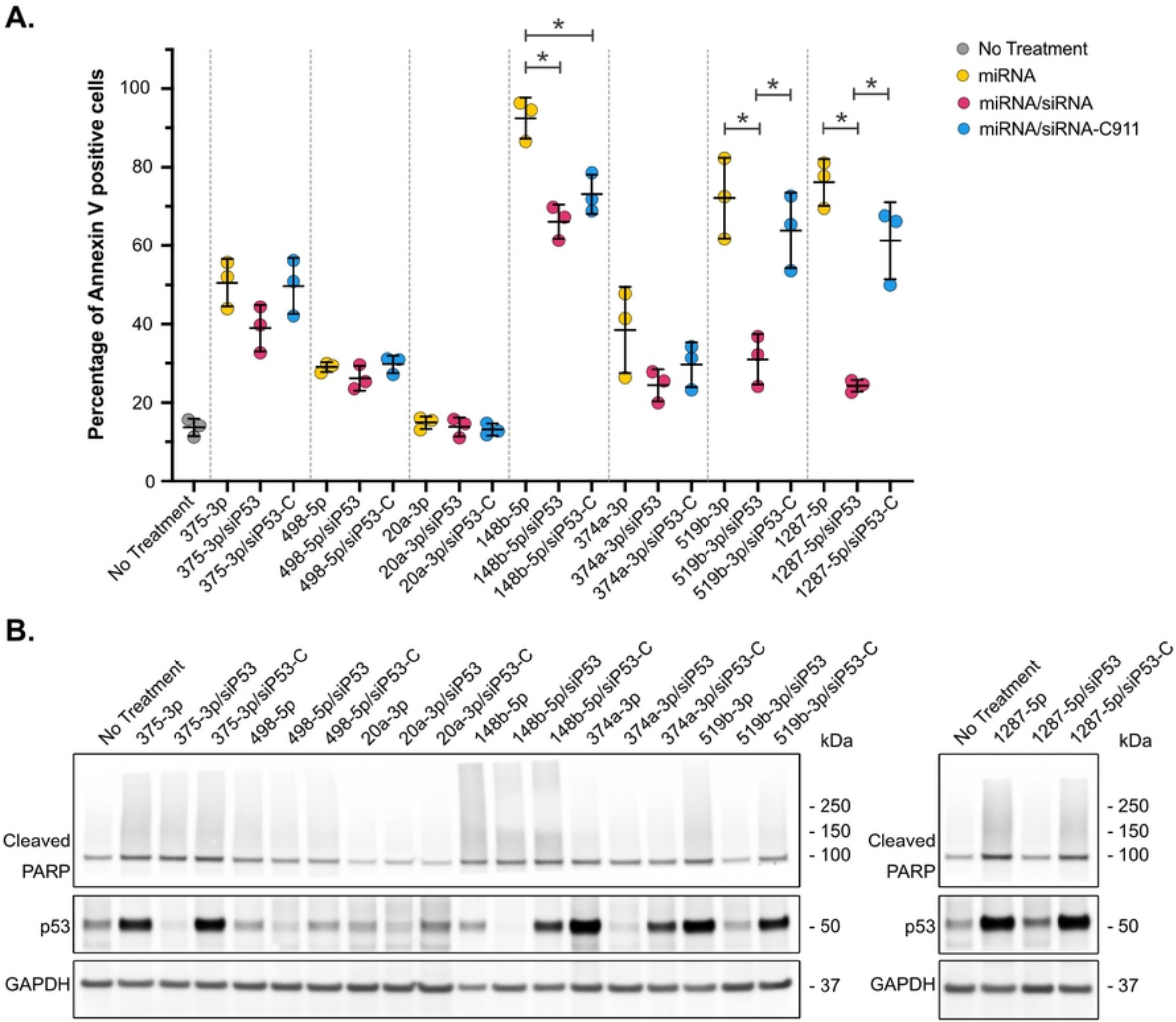
A.
Percentage of Annexin V positive cells
0
20
40
60
80
100
No Treatment
miRNA
miRNA/siRNA
miRNA/siRNA-C911
No Treatment
375-3p
375-3p/siP53
375-3p/siP53-C
498-5p
498-5p/siP53
498-5p/siP53-C
20a-3p
20a-3p/siP53
20a-3p/siP53-C
148b-5p
148b-5p/siP53
148b-5p/siP53-C
374a-3p
374a-3p/siP53
374a-3p/siP53-C
519b-3p
519b-3p/siP53
519b-3p/siP53-C
1287-5p
1287-5p/siP53
1287-5p/siP53-C
B.
kDa
Cleaved PARP
p53
GAPDH
- 250
- 150
- 100
- 50
- 37

Figure 7